Ultrasonic Testing on EUROFER Welded Joints for Determination of the Minimum Detectable Flaw Size

Final Report
TW6-TTMS-005, D5

Tatiana Martin, Stefan Knaak,
Yunlong Zhong, Jarir Aktaa

KIT Scientific Publishing

Tatiana Martin, Stefan Knaak, Yunlong Zhong, Jarir Aktaa

Ultrasonic Testing on EUROFER Welded Joints for Determination of the Minimum Detectable Flaw Size

Final Report
TW6-TTMS-005, D5

Karlsruhe Institute of Technology

KIT SCIENTIFIC REPORTS 7543

Ultrasonic Testing on EUROFER Welded Joints for Determination of the Minimum Detectable Flaw Size

Final Report
TW6-TTMS-005, D5

by
Tatiana Martin
Stefan Knaak
Yunlong Zhong
Jarir Aktaa

Institut für Materialforschung
Programm FUSION
Association Karlsruhe Institute of Technology/EURATOM

KIT Scientific Publishing

REPORT for TASK of the EFDA Technology Programme

Reference:	Field: Tritium Breeding and Materials Area: Materials Development Task: TW6-TTMS-005 Task Title: Rules for Design Fabrication and Inspection Subtask Title: Qualification of NDT (non-destructive testing) for evaluation of limits of detectable cracks. Deliverable No.: D5
Document:	Ultrasonic Testing on EUROFER Welded Joints for Determination of the Minimum Detectable Flaw Size
Level of confidentiality	Free distribution ⊠ Confidential ☐ Restricted distribution ☐
Author(s):	Tatiana Martin, Stefan Knaak, Yunlong Zhong, Jarir Aktaa Karlsruhe Institute of Technology, Germany
Date:	28 May 2010
Distribution list:	Rainer Laesser (Field Co-ordinator) Eberhard Diegele (Responsible Officer) Bob van der Schaaf (Project Leader) Farhad Tavassoli (Task Co-ordinator)
Abstract:	The ferritic-martensitic steel EUROFER is intended for use as a structural material for blanket components of future fusion reactors. A blanket module consists of a multiplicity of diffusion-welded cooling plates, which are connected by TIG, EB or laser welding seams. For the quality assurance of these welding seams the ultrasonic non-destructive testing is currently examined. In the context of this work the manual testing and the ultrasonic immersion testing are considered for the examination of EUROFER parts including welding seams of different types (diffusion welding, electron-beam welding and TIG - welding). Differently arranged artificial flaws of varying sizes were introduced into the welding seams to determine their minimum detectable size. In essence, the artificially introduced flaws for immersion testing consisted of longitudinal holes and cross holes 0.2 mm to 1.0 mm in diameter as well as of tungsten wires whose diameter was in the range of 0.2 mm to 1.0 mm. For manual testing holes were introduced with a diameter of 0.5mm only. Investigations were conducted using the KC 200 immersion testing facility developed by GE Inspection Technologies and the USD 15s by Krautkramer for manual scanning. Ultrasonic testing was performed intermitting straight- and angle beam examinations of longitudinal and transverse waves from sensors of different resolutions. The DAC (Distance Amplitude Correction) curves for flaws that are 0.2 mm and 0.1 mm in diameter were derived from the measuring results in addition.

REPORT for TASK of the EFDA Technology Programme		
Reference:	Field: Tritium Breeding and Materials Area: Materials Development Task: TW6-TTMS-005 Task Title: Rules for Design Fabrication and Inspection Subtask Title: Qualification of NDT (non-destructive testing) for evaluation of limits of detectable cracks. Deliverable No.: D5	
Revision No: -	Changes: -	
	Written by:	Revised by:	Approved by:
	Tatiana Martin	Jarir Aktaa	Oliver Kraft

Abstract

The ferritic-martensitic steel EUROFER is intended for use as a structural material for blanket components of future fusion reactors. A blanket module consists of a multiplicity of diffusion-welded cooling plates, which are connected by TIG, EB or laser welding seams. For the quality assurance of these welding seams the ultrasonic non-destructive testing is currently examined. In the context of this work the manual testing and the ultrasonic immersion testing are considered for the examination of EUROFER parts including welding seams of different types (diffusion welding, electron-beam welding and TIG - welding). Differently arranged artificial flaws of varying sizes were introduced into the welding seams to determine their minimum detectable size. In essence, the artificially introduced flaws for immersion testing consisted of longitudinal holes and cross holes 0.2 mm to 1.0 mm in diameter as well as of tungsten wires whose diameter was in the range of 0.2 mm to 1.0 mm. For manual testing holes were introduced with a diameter of 0.5mm only. Investigations were conducted using the KC 200 immersion testing facility developed by GE Inspection Technologies and the USD 15s by Krautkramer for manual scanning. Ultrasonic testing was performed intermitting straight- and angle beam examinations of longitudinal and transverse waves from sensors of different resolutions. The DAC (Distance Amplitude Correction) curves for flaws that are 0.2 mm and 0.1 mm in diameter were derived from the measuring results in addition.

Ultraschalluntersuchungen an EUROFER- Schweißverbindungen zur Bestimmung der minimalen detektierbaren Fehlergröße

Zusammenfassung

Der ferritisch-martensitische Stahl EUROFER soll als Strukturmaterial für Blanket- Komponenten zukünftiger Fusionsreaktoren eingesetzt werden. Ein Blanketmodul besteht aus einer Vielzahl diffusionsgeschweißter Kühlplatten, die miteinander durch WIG-, EB- oder Laserschweißnähte verbunden werden. Für die Qualitätssicherung der Schweißnähte wird zurzeit von den verwendeten Zerstörungsfreiprüfungen die Ultraschallprüfung untersucht. Im Rahmen dieser Arbeit wird über den Einsatz von sowohl der Ultraschall-Kontakttechnik als auch der Ultraschall-Tauchtechnik bei der Prüfung von Teilen aus EUROFER mit drei Schweißnahttypen (Diffusionsschweißen, Elektronenstrahlschweißen und WIG - Schweißen) berichtet. Die Schweißnähte dieser Teile wurden mit unterschiedlich angeordneten künstlich eingebrachten Fehlern versehen, deren Größe auch variiert wurde, um die minimale detektierbare Fehlergröße zu ermitteln. Im Wesentlichen waren die künstlichen Fehler als Senkrecht- und Querbohrungen von 0,2 mm bis 0,5 mm im Durchmesser sowie Wolframdrähte von 0,2 mm bis 1,0 mm im Durchmesser für die Tauchtechnikprüfung eingebracht. Für die Prüfungen in der Kontakttechnik wurden dieselben Bohrungen vorbereitet, allerdings nur mit einem Durchmesser von 0,5 mm. Die Kontakttechnikuntersuchungen wurden mit dem Gerät USD 15s der Firma Krautkramer durchgeführt. Die Tauchtechnik-Anlage KC 200 der Firma GE Inspection Technologies wurde für die Prüfungen in der Tauchtechnik verwendet. Die Tauchtechnikultraschallprüfung wurde mit Senkrecht- und Schrägeinschallungen von Longitudinal- und Transversalwellen aus Sensoren unterschiedlicher Auflösung durchgeführt. Aus den Messergebnissen wurden zum Schluss die DAC- Kurven (Tiefenausgleichkurven) für die Fehlergrößen 0,2 mm und 0,1 mm im Durchmesser abgeleitet.

TABLE OF CONTENTS

1 Introduction

In blanket modules, e. g. the EU Test Blanket Modules (TBMs), the low activation steel like EUROFER 97 will be used as structural material. The first wall and cooling plates with cooling channels will be welded by Hot Isostatic Pressing (HIP), and the stiff grids are expected to be welded by Electron-Beam (EB) or Tungsten Inert Gas (TIG). Welded structures can fail catastrophically if they contain cracks above a certain critical size for the load applied. Using the concepts of fracture mechanics, it is possible to determine the extent to which a pre-existing crack might propagate to an unacceptable level during service. For computation of fracture mechanics parameters like stress intensity factor, it is essential to know the exact location, configuration and the size of the cracks. Therefore, development of a Non-Destructive Testing (NDT) method to detect the cracks in the welded area is one of the key issues in developing plasma-facing components (PFCs) for next generation fusion devices. The aim of the NDT is to find in the considered components in-homogeneity or defects without their destruction and to evaluate the test results so that a decision can be made for the applicability of these components. Among the most widely used NDT techniques, Magnetic particle testing (MT), Liquid Penetrate testing (PT) and Eddy current testing (ET) can only detect the flaws on the surface of the specimen. In contrast, radiography (RT) and ultrasonic testing (UT) are the most frequently used methods of testing different test pieces for internal flaws. A detailed comparison between RT and UT can be found in the previous studies of A. Erhard, U. Ewert and I.J. Roux [1, 2]. Based on this comparison the ultrasonic testing technique was chosen in current work.

Within the reporting period the ultrasonic testing has been evaluated. This method can be used to detect surface flaws such as cracks as well as internal flaws such as voids or inclusions of foreign material. It is also commonly used to measure wall thickness in tubes and diameters of bars.

Ultrasonic testing is one of the mostly applied procedures in non-destructive materials testing (NDT). It is used for examination of welds, castings, automotive components, pressure vessels, etc. Non-destructive testing is one of the most important methods of safety monitoring. Comparable with medical diagnostics, NDT serves to detect latent defects in structures and components at an early stage before and during use, thus ensuring that unforeseen failure is avoided.

Non-destructive material testing by means of ultrasonic methods has a tradition of more than four decades. Very first examinations using ultrasonic oscillations for detection of flaws in different materials have developed into classical investigations based on measurements that take into account the entire range of important influencing factors. Today, ultrasonic testing, supported by greatly advanced instrument technologies, yields reproducible test results within narrow tolerances. This requires exact knowledge of the influencing factors and the application of such factors during testing [3].

Basic Principles of Ultrasonic Testing [4] and Non-destructive Material Testing with Ultrasonic [5] are recommended for a fundamental understanding of Ultrasonic Testing.

2 Detection of Defects in EUROFER with Manual Testing

2.1 Ultrasonic Testing

In ultrasonic testing (UT), the wavelength of the ultrasound used has a significant effect on the probability of detecting a discontinuity. A general rule of thumb is that a discontinuity must be larger than one-half the wavelength to stand a reasonable chance of being detected. As a consequence, the ultrasonic wavelength limits the minimum flaw size which can be detected. It can be determined by the following formula

$$\lambda = \frac{c}{f} \tag{1}$$

with λ, c and f denoting the wavelength, velocity and frequency of the ultrasonic wave, respectively. The velocities of longitudinal and transverse ultrasonic waves in the steel are about 5920 and 3255 m/s, respectively. Assuming a frequency of 10 MHz used in the ultrasonic testing, a detect ability of discontinuities with sizes of about 0.3 mm and 0.15 mm is determined for longitudinal and transverse ultrasonic waves, respectively. A higher frequency will increase the resolution to locate smaller discontinuities; however, the maximum depth in a material at which flaws can be located is reduced due to the scattering of the sound energy.

Since the non-destructive testing technique is very essential to monitor the degradation of first wall materials in the nuclear fusion reactor under neutron irradiation during their operation, the development of this technique is needed to maintain the integrity of materials used for structures and components such as first wall. The velocity and attenuation coefficient of both shear and longitudinal waves propagating in the specimens before and after subjecting to irradiation could be calculated to evaluate the embrittlement owing to irradiation. The propagation time between the first and the second back wall echoes, and the pulse amplitude of these echoes will be estimated from the pulse echo displayed on a CRT. The velocity and attenuation coefficient were calculated by the following equations [6]:

$$c = \frac{2T}{t_2 - t_1} \tag{2}$$

$$a = \frac{20 \log\left(\frac{h_1}{h_2}\right)}{2T} \tag{3}$$

Where c and a are the velocity and the attenuation coefficient of the ultrasonic wave, respectively. T is the thickness of the specimen; t is the propagation time of the back wall echo; h is the pulse amplitude of the back wall one. The subscripts 1 and 2 denote the first and the second back wall echoes, respectively.

2

The calibration of straight-beam probes without delay line with unknown material velocity and the calibration with angle-beam probes where material velocity is unknown are detailed described in page 5-35 and page 5-41 of Technical reference and operation manual of Krautkramer USD 15 [7], respectively. According to the steps, the velocities of longitudinal and transverse waves in EUROFER 97 can be obtained to be 5948 m/s and 3283 m/s, respectively, as shown in Fig. 1a and 1b. From Fig. 2, the attenuation coefficient of longitudinal wave in EUROFER 97 can be measured as follows:

$$a = \frac{20\log\left(\frac{h_1}{h_2}\right)}{2T} = \frac{20\log\left(\frac{89}{67.5}\right)}{2*10} = 0.12 \tag{4}$$

1a   1b
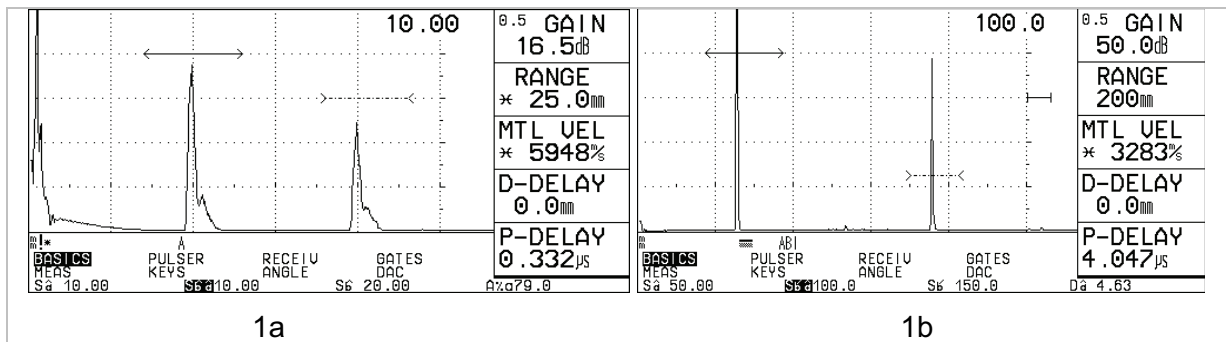
Fig. 1:   Measurement of (a) longitudinal and (b) transverse velocities in EUROFER 97
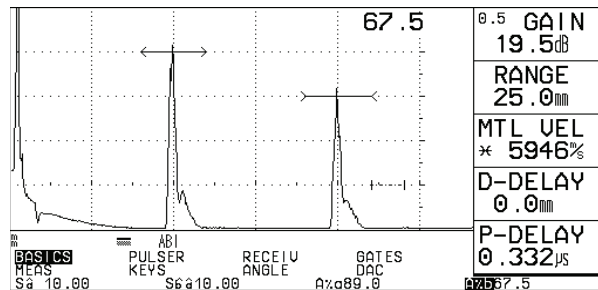

Fig. 2:   Measurement of the attenuation coefficient of longitudinal wave in in EUROFER 97

The measured velocities of the shear and longitudinal waves propagating in EUROFER 97 material are related with the elastic module of EUROFER 97 by the following equations [7]:

$$c_s = \sqrt{\frac{G}{\rho}} = \sqrt{\frac{E}{\rho}\frac{1}{2(1+\upsilon)}} \tag{5}$$

$$c_l = \sqrt{\frac{K + (4/3)G}{\rho}} = \sqrt{\frac{E}{\rho}\frac{1-\upsilon}{(1+\upsilon)(1-2\upsilon)}} \tag{6}$$

Where G, E and K are the shear, Young's and bulk module, respectively. ρ and v are the density and Poisson's ratio, respectively.

Since c_l and c_s are known and adopting ρ as 7750 kg/m^3 for EUROFER 97 [9], E, G, K and v can be calculated from Equations (5) and (6).

E, GPa	υ	G, GPa	K, GPa
213.4	0.28	83.4	163

The Young's modulus E is 213.4 GPa, which is very near to the value of 217 GPa for F82H steel. The Poisson's ratio v is determined equal 0.28 which is different from the value of 0.3 used for EUROFER 97 in [8].

2.2 Examination of Defects in EUROFER with Manual Ultrasonic Testing

Two identical samples with dimension of 70mmx40mmx12mm were welded by TIG and by EB. Two artificial holes and one artificial hole with a diameter of 0.5 mm were drilled with an angle of 45° at the welded area and at the bottom of the TIG specimen, respectively, as shown in the sketch in Fig. 3.

Fig. 3:   Sketch of TIG (EB) specimen.
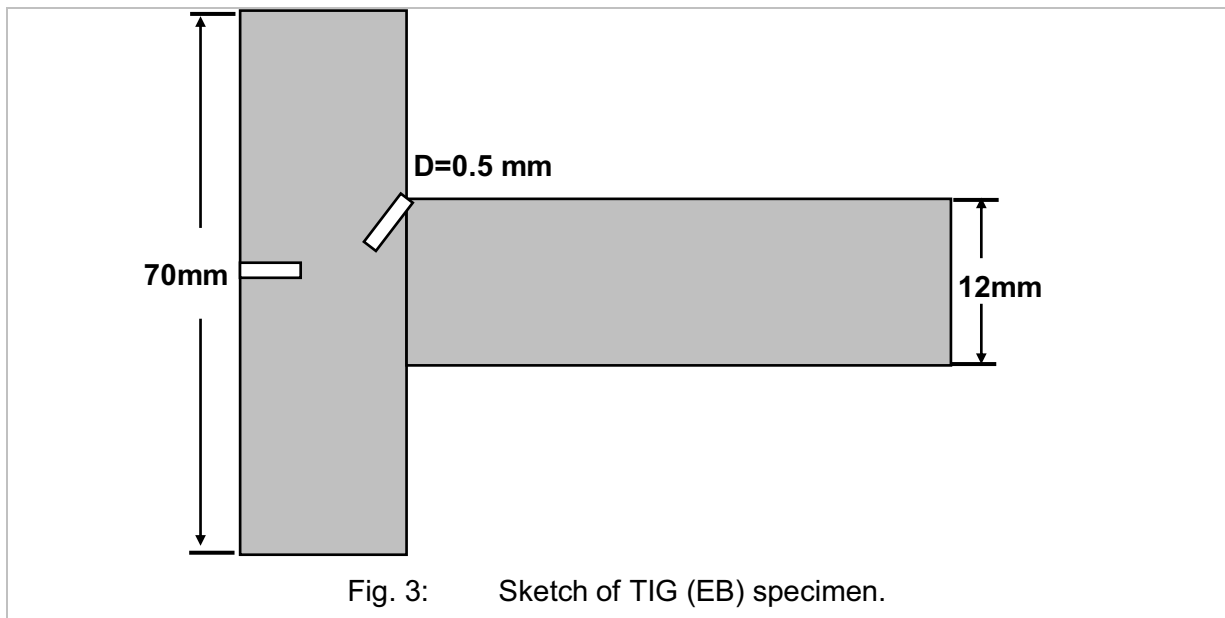
UT investigations on the TIG specimen were conducted by GE Inspection Technologies, and the results are given in Annex A (specimen 1) and Annex B. Similar and independent experiments were also done at FZK with USD 15s and probes K15K and MSW-QC 10. It can be clearly seen from Fig. 4 that there is only an echo reflected from the back wall of the specimen at the position 1, whereas another echo reflected from the artificial hole is shown in

the middle of the screen. To detect the artificial holes drilled at the welded area, angle beam probe is used. The principle is given in Annex B. As illustrated in Fig. 5, obvious echoes are reflected from the artificial holes, and the positions of the holes can be determined according the data provided from UT tests. The positioning of hole 1 (see Fig. 5) in the TIG specimen is sketched in Fig. 6, where S_a, D_a, R_a are time of flight for gate A, depth for gate A and reduced projection distance for gate A, respectively. More details about the data explanation can be found in pages 5-18, 19, 24 of Reference 7.

Fig. 4:   Results of UT on the bottom hole of the TIG specimen with probe K15K.
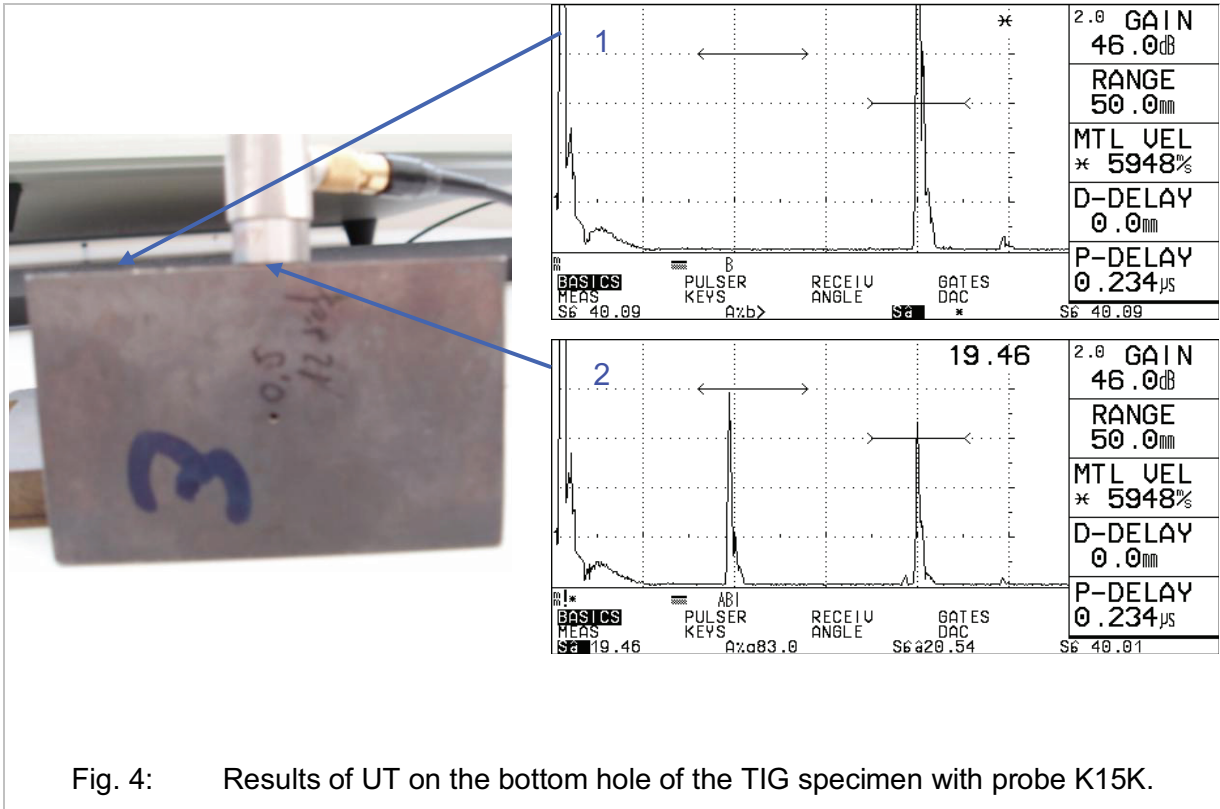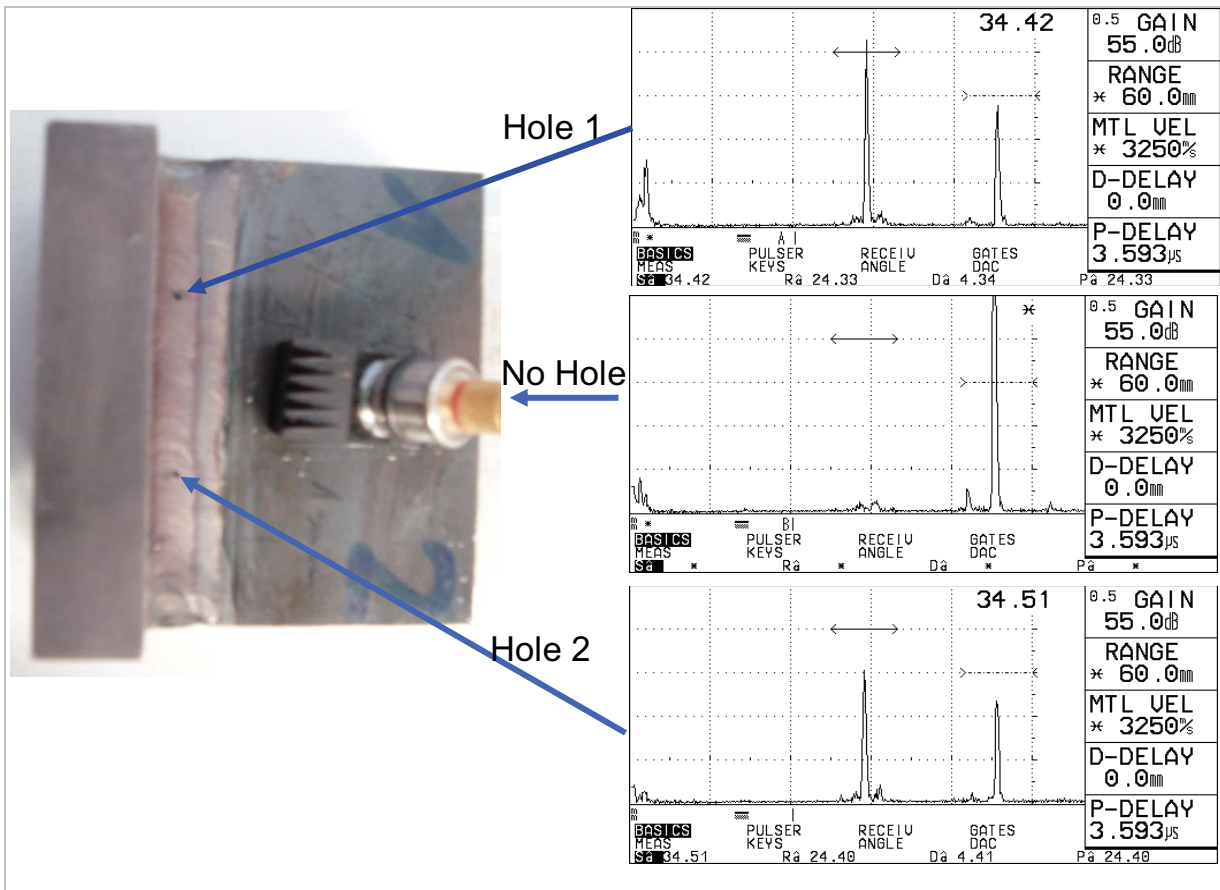
Fig. 5:   Results of UT on the artificial holes at the welded area by angle beam probe.
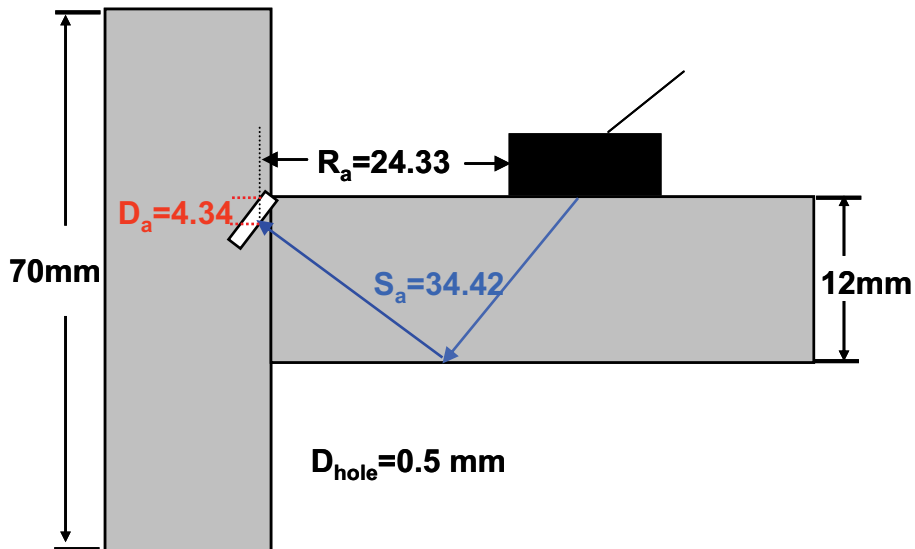

Fig. 6:   Positioning of the hole 1 in the welded joints of TIG specimen.

A specimen fabricated by diffusion welding with cooling channels was drilled with some holes with diameters ranging from 0.4 to 1 mm, as sketched in Fig. 7. It was detected by USD 15 and USM35 with probes IAP 10.6.3 and H15MN20 by immersion testing with C-Scan at GE Inspection Technologies. The results are given in Annex A (specimen 2). It can be seen that all the holes from 0.4 to 1mm could be detected with the 10MHz probe, while with 15 MHz probe a higher resolution could be obtained. Judging from the colour map in the Fig. 7 in Annex A, it becomes clear that the 15 MHz probe could at least detect a hole with a diameter of 0.3 mm.

Fig. 7:   Specimen and sketch of Automated Ultrasonic Testing.
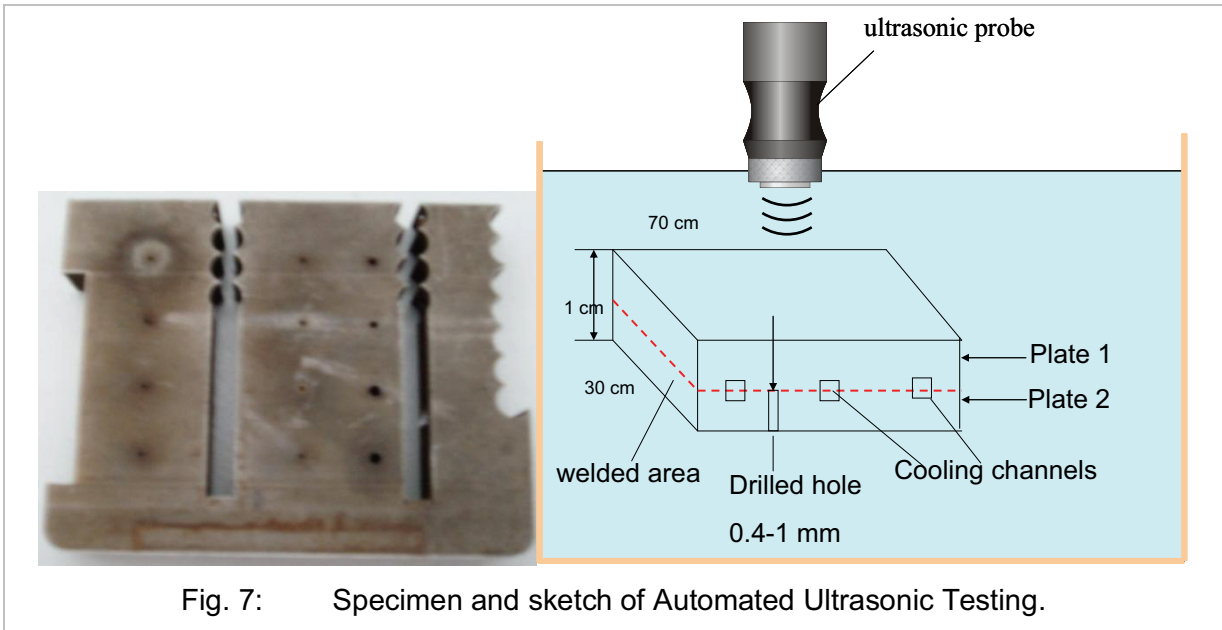
The artificial discontinuity with known size could be best evaluated by accurately knowing the "real reflector size", therefore, it is expected that ultrasonic testing can give this information. However, because the reflected sound coming from the discontinuity is interpreted as the echo on the display, it is very often difficult, and in some cases even impossible, to reliably assert the size of the reflector. In fact, the echo height plays the decisive part when evaluating discontinuities during manual ultrasonic testing. The so called DSG scales should be obtained for the probes evaluating the EUROFER 97 materials. DGS means that the scale is allocated an echo at the Distance, with correctly set Gain and Size. An example of the probe B4S is shown in Fig. 8.

Fig. 8: DGS scale for the probe B4S.
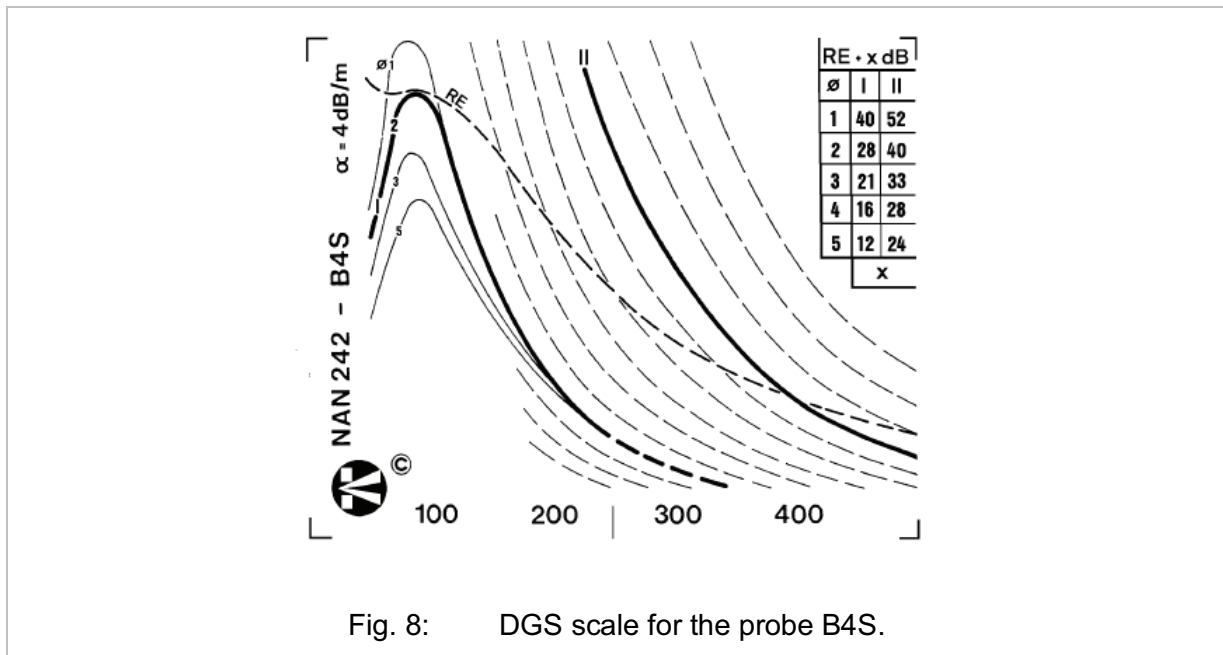
For further manual testing, a reference block made of EUROFER 97 material was fabricated with different discontinuities. Their maximum echo heights marked on the attachment scale of the display and joined by a curve. The curve produced is called the DAC curve (distance amplitude correction) - the distance referenced loss compensation, as shown in Fig. 9. When a discontinuity echo appears, an immediate assessment can be made whether or not the discontinuity echo exceeds the DAC. In addition to this a determination is made, by a corresponding gain change, to see by how many dBs an echo exceeds the curve. This excess recorded echo height is the reproducible measure for the evaluation and reporting of the discontinuity.

Fig. 9: DAC of the reference echoes.
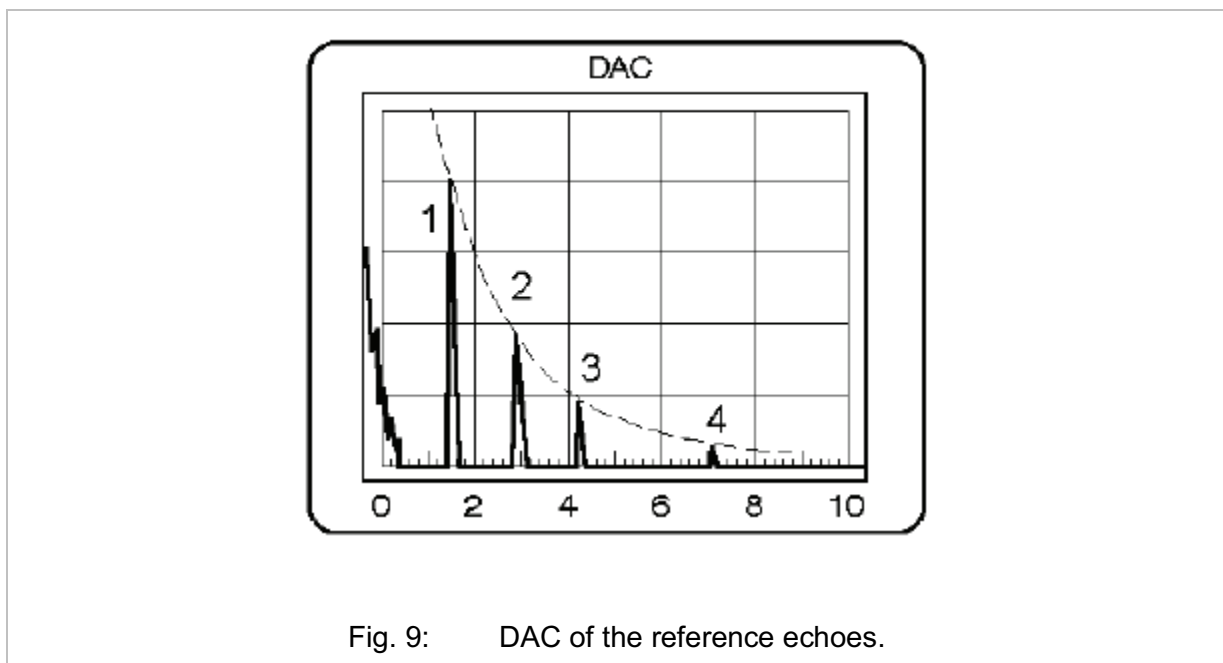
3   Determinations of the Flaw Size in EUROFER with Immersion Testing

3.1   Immersion Testing

The immersion ultrasonic testing is one of the ultrasonic testing techniques used for the quality control of welds. The space between search unit and work piece must be relatively large and be filled completely with a liquid coupling medium (e.g. water). Immersion technique is characterized by the fact that coupling operations are optimal. Covering the shortest dead zones, this technique is optimal for local and remote resolving. Although any liquid may be used, water is preferred for most applications. Depending on the individual requirements, corrosion-protective agents or wetting agents which decrease the surface tension may be added. The distance between search unit and test specimen must be selected in such a way that the echoes are clearly separated from the work piece by the repetitions of the surface echo. For a complete examination, either search unit or work piece must be moved while the selected sound direction is kept constant [10].

3.1.1   Straight -Beam Examinations

SI: Transmission puls
OE: Surface echo
RE: Back wall echo
FE: Flaw echo

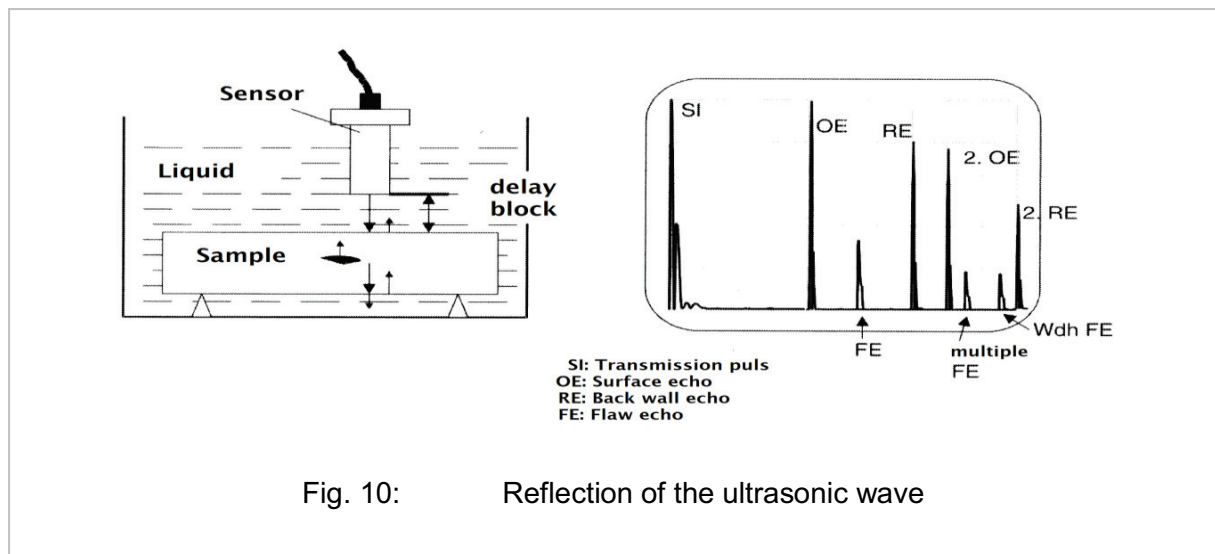Fig. 10:   Reflection of the ultrasonic wave

Fig. 10 shows the connection between the reflections of the ultrasonic wave at the surface and inside of the specimen and the signals received from the search unit. After having passed the so-called "water delay block", part of the wave at the interface between water and specimen is reflected and returned back to the transducer. This so-called entrance echo appears on the fluorescent screen as the first echo after the transmission impulse [11]. The entrance echo is used for adjustment of the position of the immersion testing probe. When the sound beam meets the material surface exactly perpendicularly, the entrance echo reaches its maximum amplitude. In the case of a homogeneous material, the next reflection at first occurs on the back surface of the specimen. This phenomenon is referred to as back-wall echo. The sound portion penetrating the work piece produces a back-wall echo se-

quence when the work piece is coplanar. In the presence of internal boundary surfaces (e.g. grain boundaries, pores, layers, or defects), part of the wave is reflected back before a back wall echo, so-called flaw echo appears. Repeat ranges also form in the presence of the delay block. The ultrasonic device, therefore, must be adjusted in such a way that at least a first back-wall echo is emitted from the specimen before the second entrance echo appears. In the case, if the second entrance echo appeared before the first back-wall echo from the work piece, a sure interpretation of the echo indication would be not possible (Fig. 11). The length of the "water delay block" should be chosen therefore such that the above mentioned conditions are fulfilled. The adjustment range is always selected for the material that is being tested. Therefore, the value of the water delay block is related to the ratio of the sound velocity:
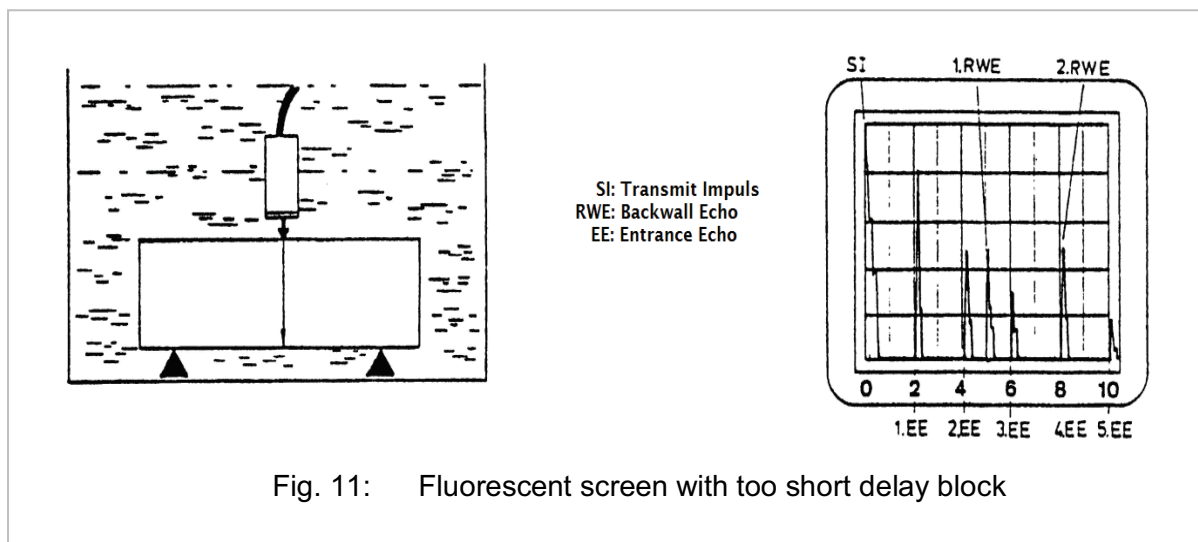
$$s_w = \frac{c_w}{c_{st}} s_{st} \qquad (7)$$

where: s_w – water delay block,

c_w – sound velocity for water,

c_{st} - sound velocity for material (steel),

s_{st} - sound path in the material (distance between first and the second entrance echo in the material) [10].

Fig. 11:   Fluorescent screen with too short delay block

Often, smaller flaws have to be detected within a given low range of depth. For optimal problem solution and a maximum reflector echo with particularly good resolution, the focus of the sound beam should be precisely within that range. For probes used for immersion testing, the focus distance (= near-field length) is indicated in water path mm.

10

The near-field lengths in steel and in water are linked with each other by the respective speeds of sound:

$$N_w c_w = N_{st} c_{st} \tag{8}$$

where: N_w – near-field length in water (focus distance);

N_{st} – near-field length in steel;

c_w – speed of sound for water;

c_{st} - speed of sound for material (steel)

Hence, for the near-field length N (St) in steel it follows that:

$$N_{st} = \frac{c_w}{c_{st}} N_w \tag{9}$$

The near-field is located partly in the water and partly in the steel. The water delay block must have a length of s_w. The part of the near-field that is identified by s_{st} (a predetermined depth to test smallest reflectors) is still located in the steel.

It follows that:

$$\frac{s_w}{N_w} + \frac{s_{st}}{N_{st}} = 1 \tag{10}$$

Solving this equation after s_w, we obtain [10]:

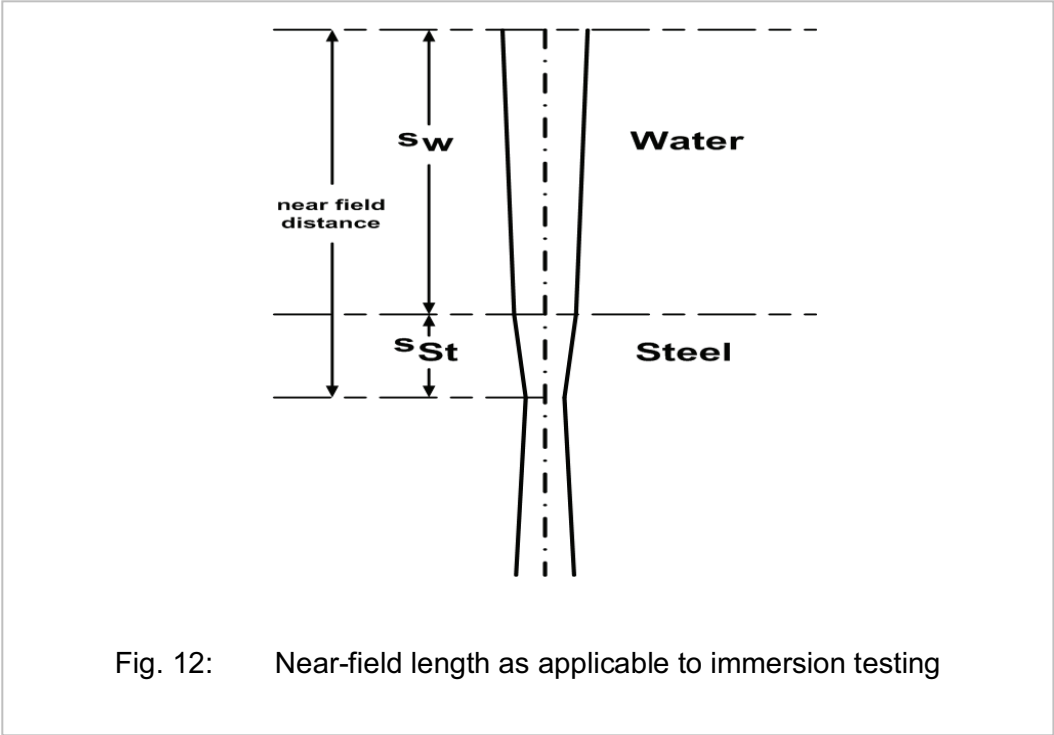$$s_w = N_w \left(1 - \frac{s_{st}}{N_{st}}\right) \tag{11}$$

Fig. 12:   Near-field length as applicable to immersion testing

3.1.2 Focusing Immersion Probes

To achieve an even better resolution and a higher sound pressure at predetermined depth ranges, one frequently applies a focusing immersion probe. Focusing is achieved mainly by means of a set of spherical lenses placed in front of the transducer. Another possibility is to use curved transducers. By focusing the near-field distance become shorter and reduces the focus width in the same proportion. The abbreviated near-field length is called a focus distance F. The proportion from the focus distance F to the real near-field (without focusing) N is characterized as the focusing degree K:

$$K = \frac{F}{N} \qquad\qquad (12)$$

with: F – focus distance,

                N – near field length of the transducer without ancillary lens

The factor K is always smaller than 1, i.e. only shortening of the focus distance can be achieved by means of the ancillary lens. One mainly uses the transducer whose focusing degree is in the range of 0.2 to 0.5. There are two kinds of focusing immersion probes, i.e. point-focusing and line-focusing ones. For line-focusing probes –here a focus has a form of a long elongated ellipse- the scanning field is broader in the work piece so, that the specimen with a broader scanning trace could be examined. The long-range flaws, for example cracks, which are oriented in the direction of the long axis of the sound beam profile, are proved optimally with the line-focusing probes. With point-focusing probes the highest sensitivity within a small, circular range of the bundle could be achieved.

Fig. 13:   Focusing of immersion probes
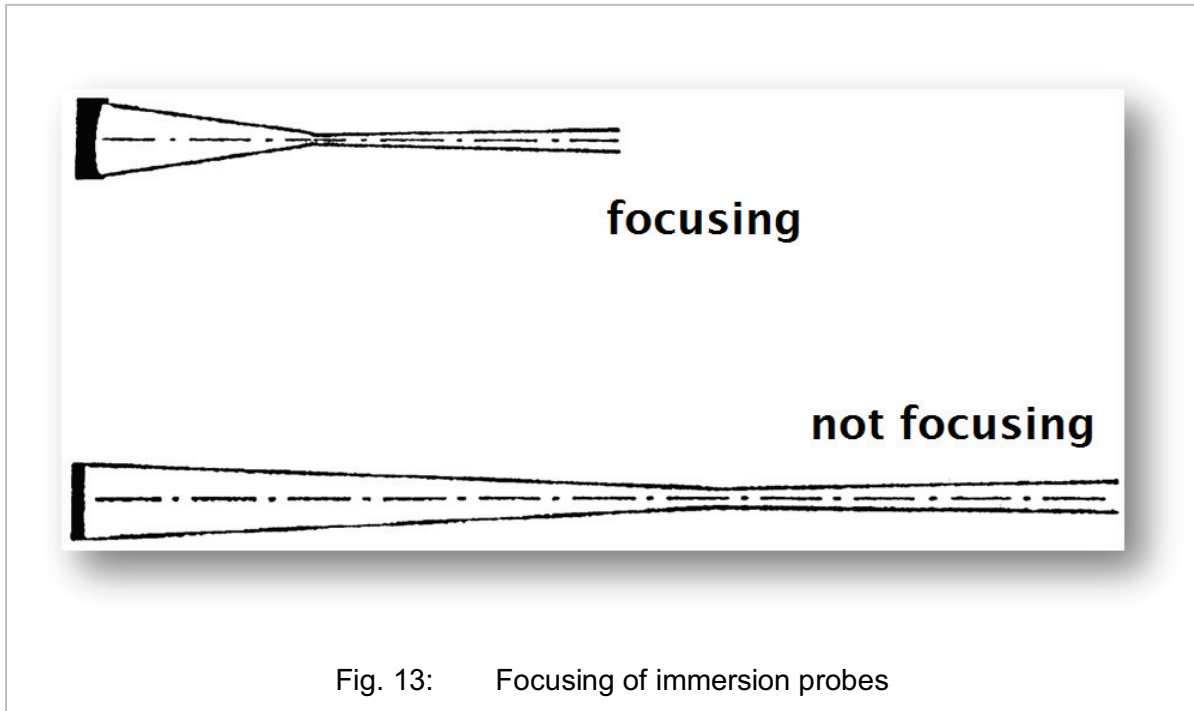
During immersion testing of a work piece the transducer is moved in its holder over the entire test surface to examine the specimen completely.

3.1.3 Angle Beam Examination

For angle beam examinations during immersion testing, probes are mounted in a holder (manipulator), considering a predetermined incident angle to the work piece surface. On the boundary surface water/test part all kinds of wave can be excited in the test specimen. To calculate the angle of incidence, one must know the sound velocities of the appropriate kinds of waves in the water as well as in the specimen. The computation law for the setting angle α (w) of the immersion probes is as follows:

$$\sin(\alpha_w) = \frac{c_w}{c_{st,tranversal}} \sin(\beta_{st}) \qquad (13)$$

where: c_w – sound velocity for water;

$c_{st,tranversal}$ – speed of sound for material for transverse waves;

β_{st} – intromission angle in material (steel)

Since the sound velocity in water is highly temperature-dependent, the water temperature must be kept almost constant during testing to avoid changes in the sound angle β [10].
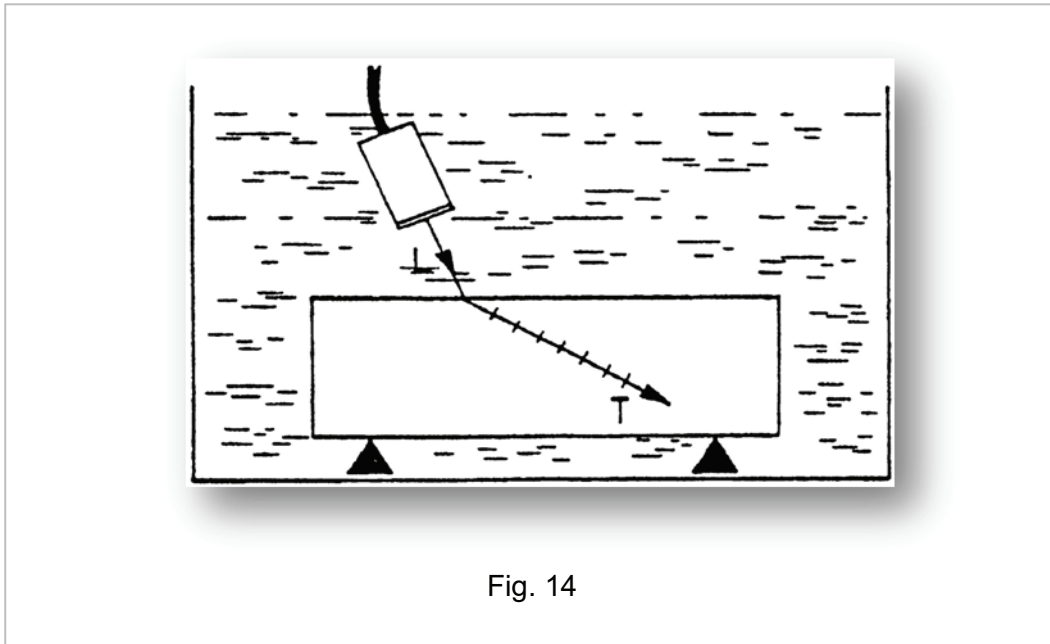
Fig. 14

3.1.4 Distance Amplitude Correction (DAC)

Distance loss compensation, i.e. DAC (Distance Amplitude Correction) curves allow an easy evaluation of reflectors, since echo heights are related to the DAC curve (echo height = DAC ± ΔdB).

Acoustic signals from the same reflecting surface will have different amplitudes at different distances from the transducer. Distance amplitude correction (DAC) provides a means of establishing a graphic 'reference level sensitivity' as a function of sweep distance on the A-scan display (time of dependence of the amplitude of the ultrasonic wave recorded by the sensor). The use of DAC allows signals reflected from similar discontinuities to be evaluated by correlating signal attenuation with flaw depth. Most often DAC will allow for loss in amplitude over material depth (time), graphically on the A-scan display but can also be done electronically by certain instruments. Because near-field length and beam spread vary according to transducer size and frequency, and different materials are characterised by different attenuation and velocity, a DAC curve must be established for each different situation. DAC may be employed in both longitudinal and shear modes of operation as well as either contact or immersion inspection techniques [12].

A DAC curve is constructed from the peak amplitude responses and from reflectors of equal area at the different distances in the same material. A-scan echoes are displayed at their non-electronically compensated height and the peak amplitude of each signal is marked on the flaw detector screen or, preferably, on a transparent plastic sheet attached to the screen. Reference standards which are commonly used are side-drilled holes (SDH), flat-bottom holes (FBH), or notches whereby the reflectors are located at varying depths. It is important to recognize that the type of reflector to be used, the size and shape of the reflector must be constant [13].

The difference between the reflector echoes for flaw evaluation is shown in the table 1.

	Distance	Size
SDH	9dB	3dB
FBH	12dB	12dB

Table 1:Difference between the reflector echoes for flaw evaluation.

Using the decrease in amplification of the DAC curve for appropriate reflectors that is shown in the table (Fig. 15), and by generating several DAC curves (a multi-DAC curve), also very small flaws can be evaluated by way of calculation. Each curve that follows identifies the flaws as having half the size of the former.

3.2 Examinations of Defects in EUROFER with Immersion Testing

Three types of welding seams (i.e. seams obtained by diffusion welding, electron-beam welding, TIG welding) with differently arranged artificial flaws were examined. The simulated flaws

consisted of longitudinal holes and cross holes with diameters ranging from 0.2 mm to 1.0 mm and tungsten wires of 0.2 mm to 1.0 mm in diameter. The experiments were performed applying straight- and angle beam examination methods activating longitudinal and transverse waves by varying the resolutions of the sensors. Eventually, the DAC (Distance Amplitude Correction) curves for flaw sizes between 0.2 mm and 0.1 mm in diameter were obtained on the basis of the transverse wave examinations.

The specimens were tested using the KC 200 immersion testing facility developed by the GE Inspection Technologies (Fig. 15).

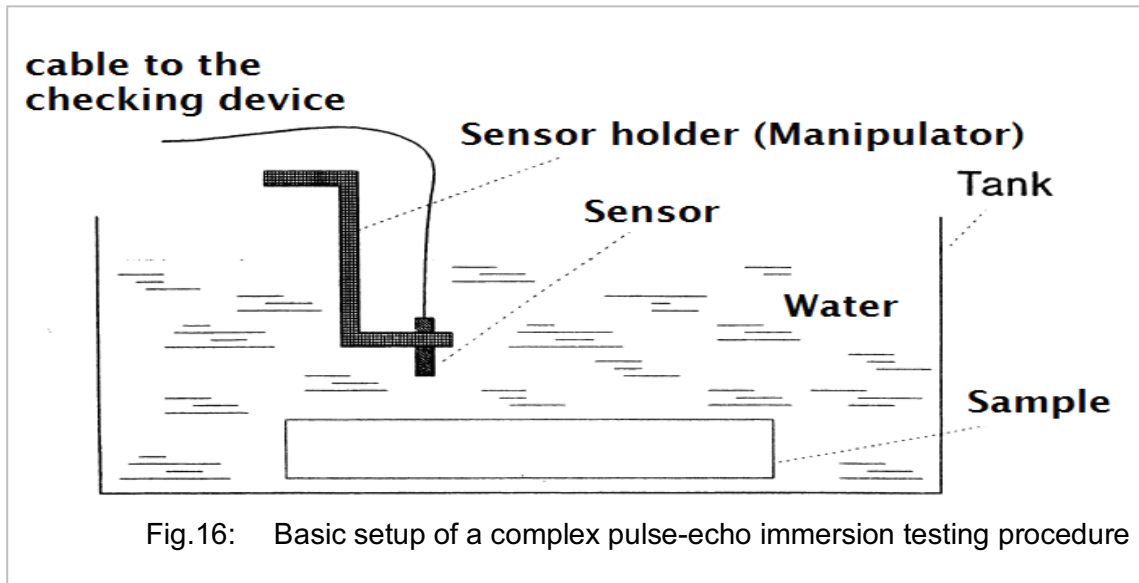Fig. 15:   Immersion testing facility KC-200

Fig.16:   Basic setup of a complex pulse-echo immersion testing procedure

The facility KC-200 includes a USIP 40 device, a KC-tank, and K-Scan software. The tank is provided with motorized X-, Y- and Z-axes and a water filter system. In addition, the system is equipped with a rotating unit. Fig. 16 shows the basic setup of a complex pulse-echo immersion testing procedure.

The specimen and transducer are immersed in a water bath. The probe is attached to a manipulator (X-, Y-, and Z-axis) which serves to scan the specimen using a USIP 40 analogue pulse-sound device. Transducers (and cable connections) for immersion testing are waterproof. Instead of being provided with a protective layer or wear zone, the immersion testing probe only has a thin delay block made of a plastic material. The probe has a simple, usually cylindrical housing that fits into a holder. This is an essential requirement for constant sound manipulation [10].

Time of dependence of the amplitude of the ultrasonic wave recorded by the sensor is referred to as the A-scan ("A-scan") (Fig. 10). The B-picture ("B-Scan") shows the signal height points as density (color coding) depending on time and on a sample coordinate. This is known from echo sounders, which provide "acoustic cross-sections". The C-picture ("C-Scan") gives an X-ray-type projection of the acoustic structure of the scanned test area (Fig. 17).
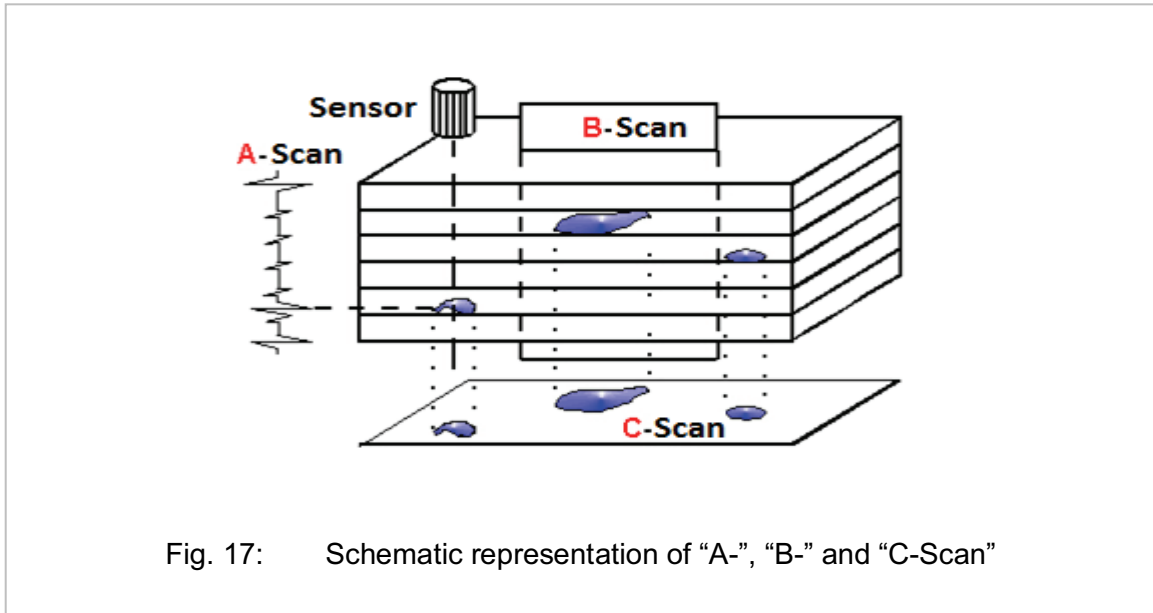
Fig. 17:   Schematic representation of "A-", "B-" and "C-Scan"

3.2.1 Diffusion Welding

Straight-beam examinations of the diffusion-welded samples were performed using a 25 MHz point-focused sensor (type IAP-25.3.1) for detection of flaws of different geometries and diameters (cross- and longitudinal holes). Therefore, three identical welded specimen of constant bottom thickness (4 mm) and variable upper part thicknesses (19 mm, 8 mm, 4 mm) and a sample of equal thickness of upper and bottom parts (5 mm) were chosen for the experiments (Fig. 19). Amplifications of 88 dB and 92 dB were chosen during testing.
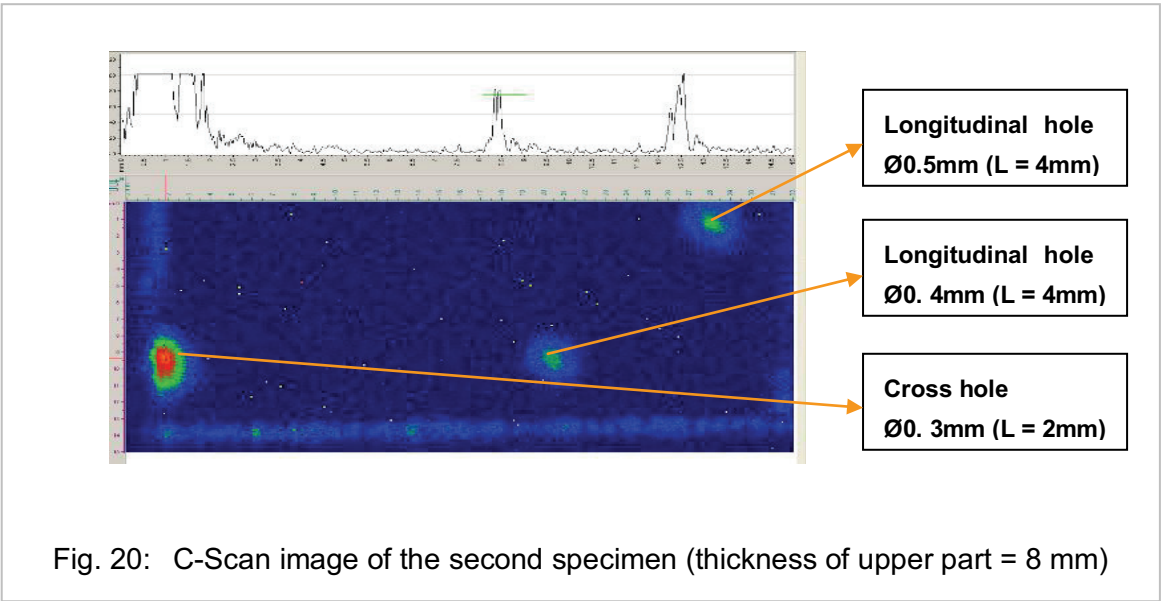

Fig. 18:   Diffusion-welded samples

Fig. 19:   C-Scan image of the first specimen (thickness of upper part = 19 mm)
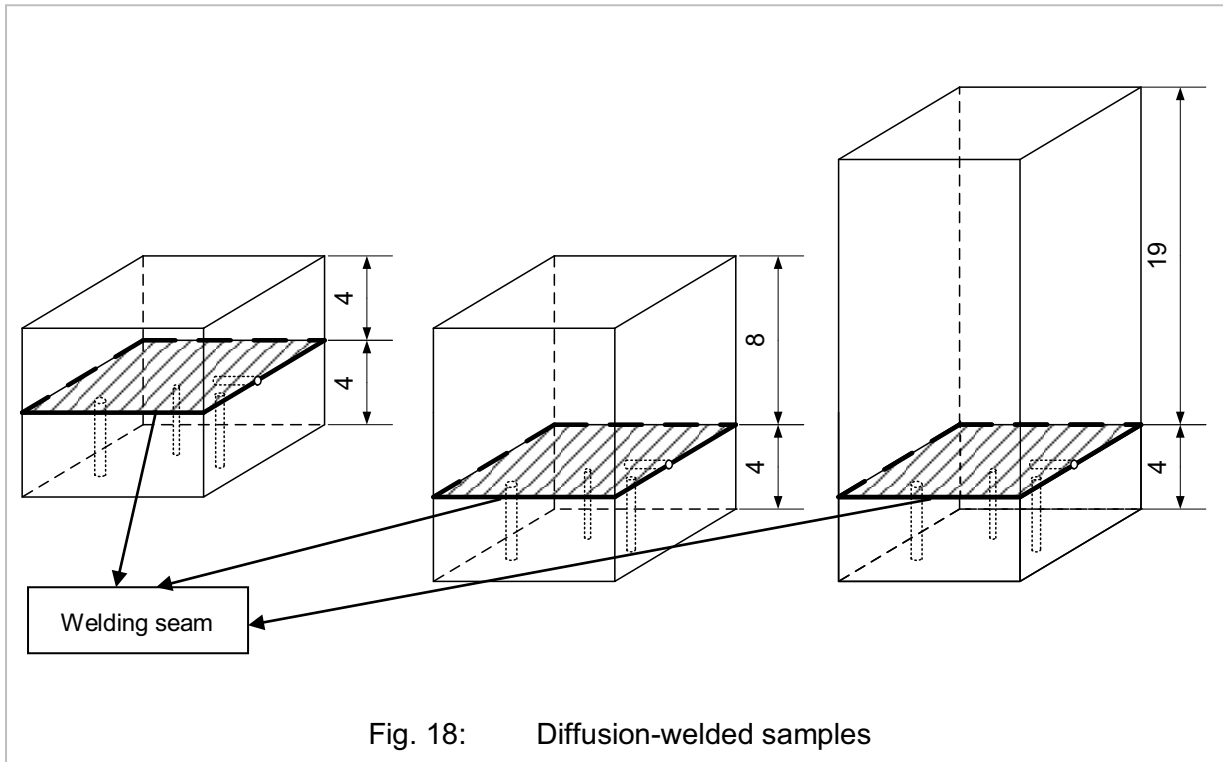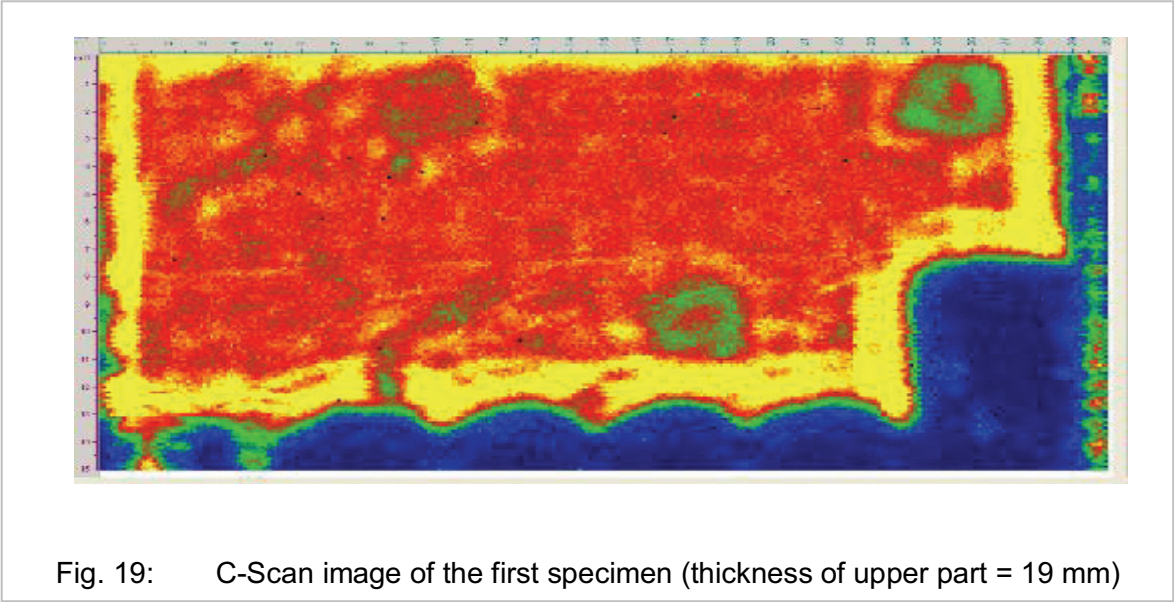
In the first specimen (thickness of upper part = 19 mm), all holes were invisible in spite of an amplification of 92 dB and an adjusted focusing depth (focus = 4 mm in the material and still 15 mm away from the welding seam). Holes contours can be detected only with the screen moving till the back wall echo (Fig. 19).

In the case of the second sample (thickness of upper part = 8 mm), the focusing depth was changed from about 1.5 mm to about 4 mm in the material at an amplification of 92 dB. With a focus adjustment of about 5 mm relative to the welding area (3 mm in the material), the longitudinal holes Ø 0.5 mm (L = 4 mm) and Ø 0.4 mm (L = 4 mm) and also the cross hole Ø 0.3mm (L = 2 mm) could be well identified and measured (Fig.20). However, the hole that was 0.3 mm in diameter and no more than 2 mm deep remained invisible due to technical reasons.

Longitudinal hole
Ø0.5mm (L = 4mm)

Longitudinal hole
Ø0. 4mm (L = 4mm)

Cross hole
Ø0. 3mm (L = 2mm)

Fig. 20:   C-Scan image of the second specimen (thickness of upper part = 8 mm)

In the third sample (thickness of upper part = 4 mm), the longitudinal holes Ø 0.5 mm (L = 4 mm) and Ø 0.4 mm (L = 4 mm) and the cross hole Ø 0.3 mm (L = 2 mm) were very clear and correctly measurable at an amplification of 88 dB and with focusing on the surface (Fig. 21). The longitudinal bore Ø 0.3 mm (L = 2 mm), however, was still invisible at a focus adjustment like that. When a higher amplification (92 dB) was selected and the focus of the sensor was inserted deeper into the sample (about 2 mm into the material, 2 mm away from the welding seam, and 4 mm relative to the drilling ground), the result was positive and even a small flaw was detected (Fig.22).
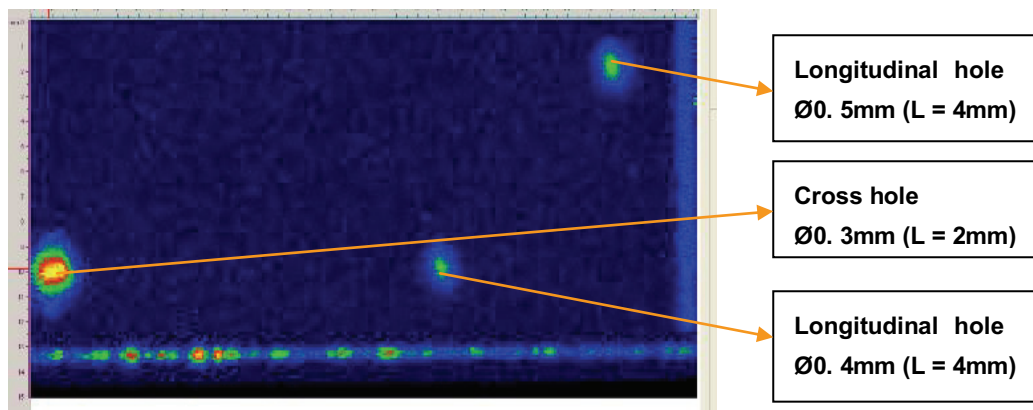
Fig. 21:   C-Scan image of the third specimen (thickness of upper part = 4 mm) with focusing on the surface
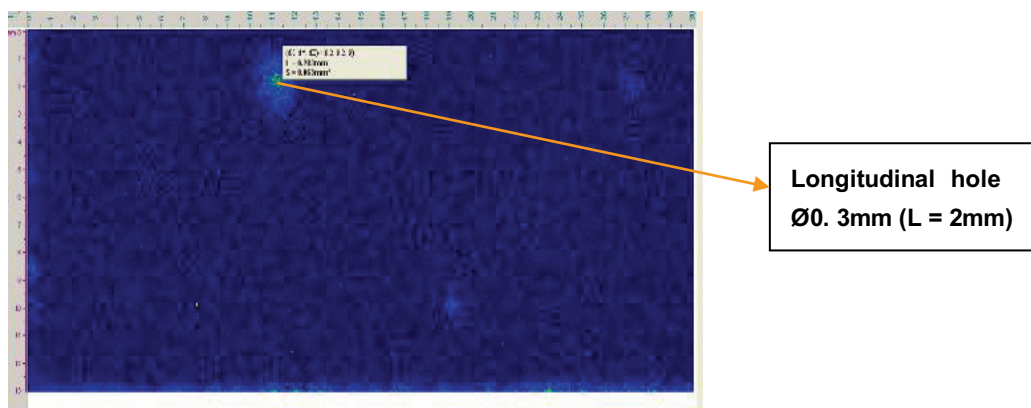

Fig. 22: C-Scan image of the third specimen with the focus about 4 mm to the drilling ground

In addition to the holes, two transverse slots with widths of 0.2 mm and 0.1 mm were inserted in a 10 mm thick sample (5 mm - upper section and 5 mm - lower part) on the lower plate to simulate cracks at an amplification of 88 dB. The C-scan reveals that a strong dispersion is emitted from these slots (Fig. 23). It is difficult, therefore, to determine their widths.

For measurement, amplification was adjusted in such a way that the simulated flaws (i.e. the holes and slots) provided the maximum possible echoes. As a consequence, the A-scan revealed the dependency of the echo maximum on the amplitude (in %) that is highlighted in colour palette, thus enabling evaluation of the indication of the echo with regard to the range of the flaw.

Fig. 23: C-Scan image of the sample with two transverse slots
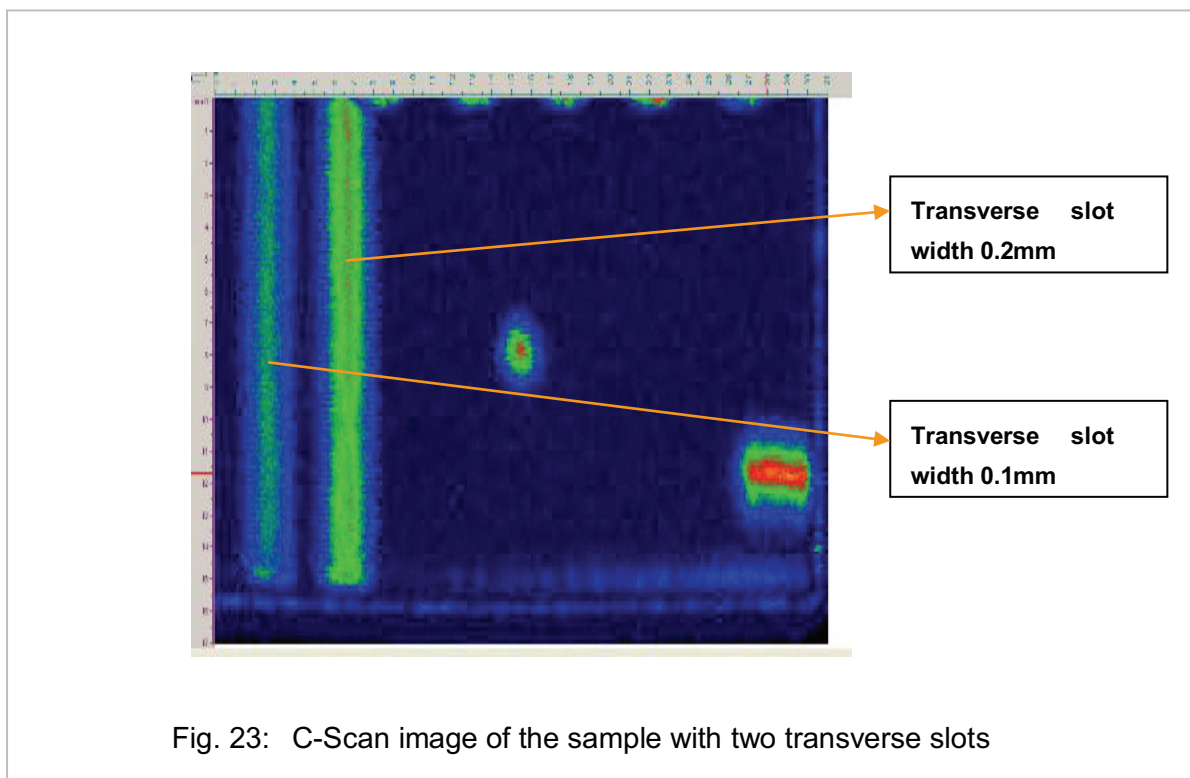
3.2.2 Electron-Beam Welding

Electron-beam welded specimen were provided with stub-welded seams, L- and T-shaped seams using two EUROFER plates with different kinds of artificial flaws such as holes, tungsten wires (1.0 mm in diameter), and graphite leads (0.5 mm in diameter) inserted within and outside of the welding range. All tests were performed using a point-focused 15 MHz transducer (type ISS).

In the case of the stub-welded sample, the tungsten wire (1.0 mm in diameter and 10 mm in length) and the graphite lead (0.5 mm in diameter and 10 mm in length) were directly introduced into the welding seam. Using different angles of incidence (α_w = 10 and 19°) and applying longitudinal and transverse waves, the artificial flaws could be identified. While the tungsten wire (1.0 mm in diameter and 10 mm in length) was very well visible and measurable independent of the setting angle (Fig. 24), the graphite lead (0.5 mm in diameter and 10

mm in length) could not be detected, probably because it had been broken during welding). The experiments were performed at an amplification of 85 dB.
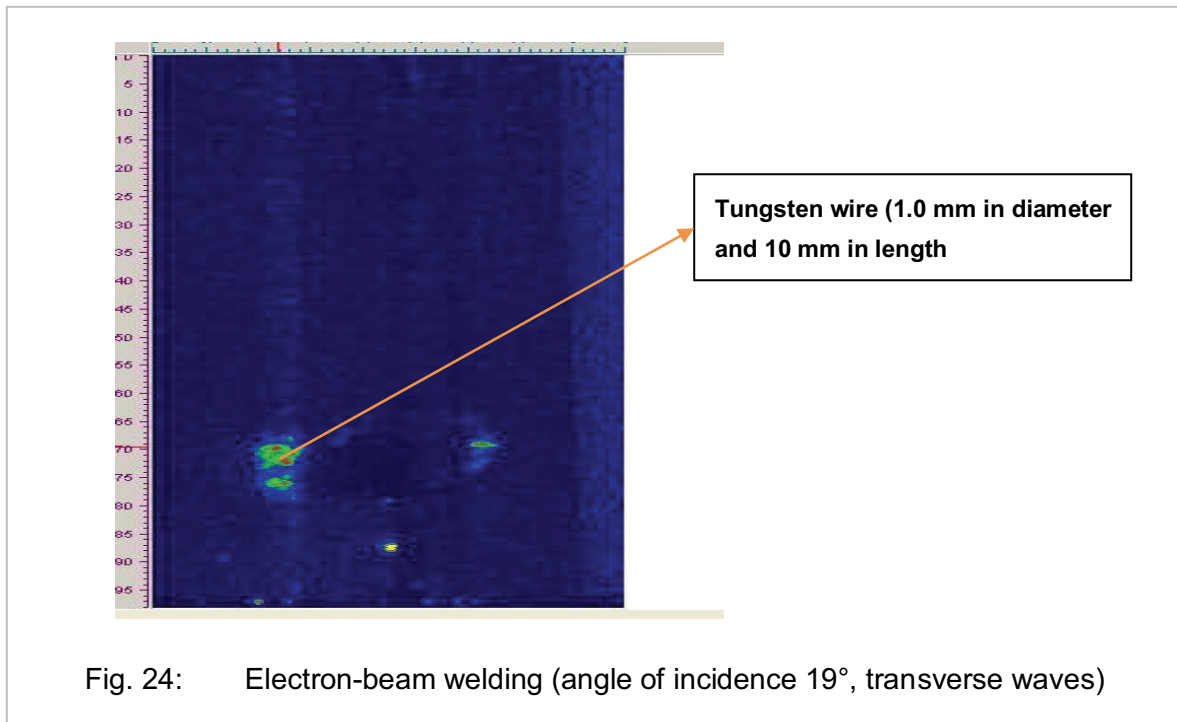

Fig. 24:   Electron-beam welding (angle of incidence 19°, transverse waves)

The next part examined was the L-welded sample having three cross holes (0.55 mm in diameter and 6 mm deep) in and outside of the welding seam. The holes (one - in the material and two - within the welding range) were drilled in different cut layers with intervals of 20 mm (Fig 25).
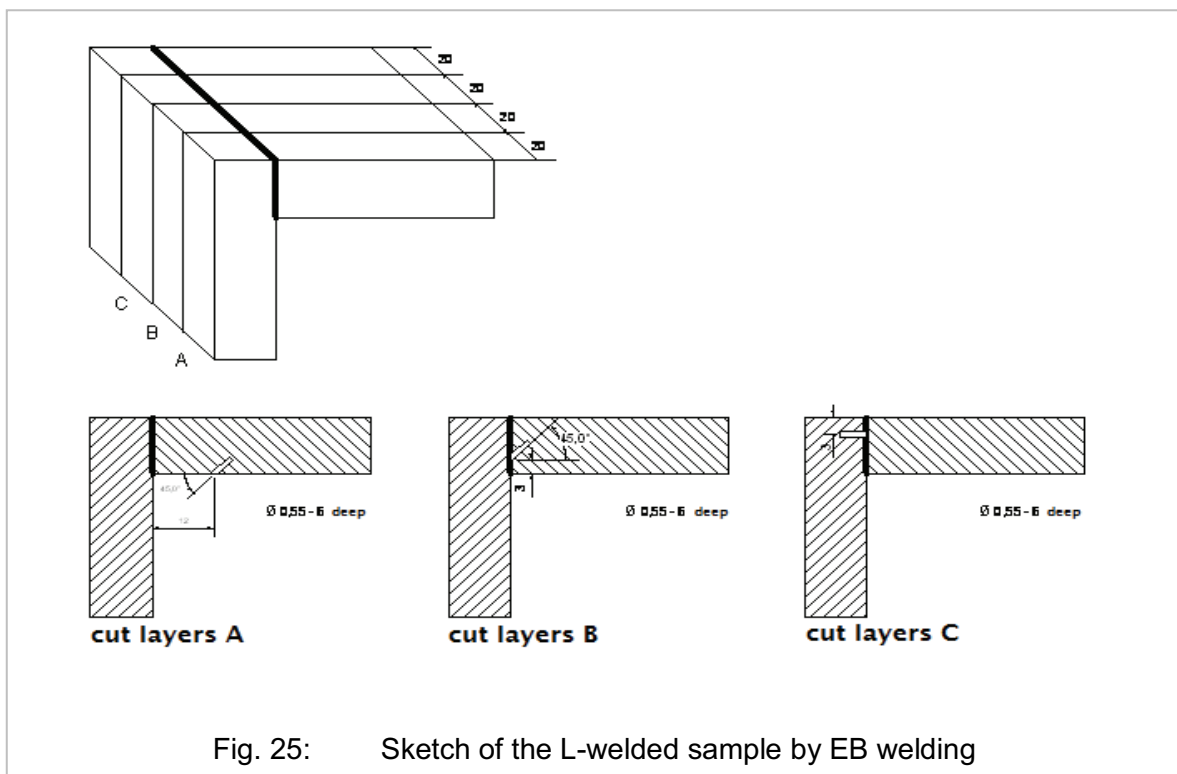
Fig. 25:   Sketch of the L-welded sample by EB welding

Choosing a setting angle of α_w = 19° with transverse waves and changing the positioning of the specimen, all three artificially inserted holes could be rather well identified at an amplification of 80 – 82 dB (Fig. 26).
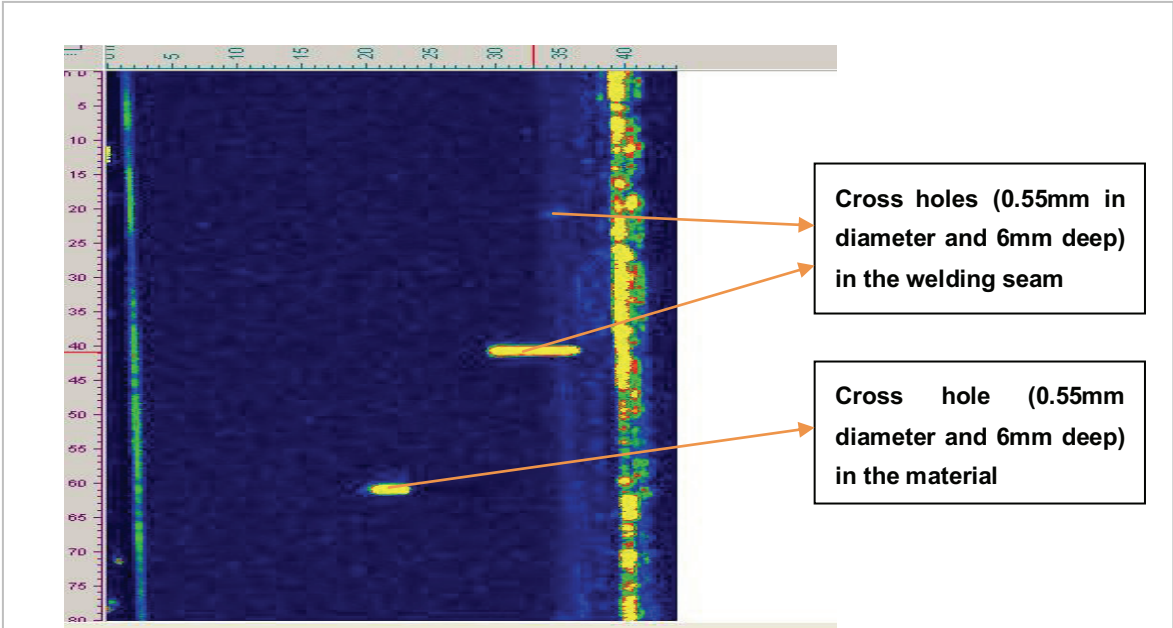

Cross holes (0.55mm in diameter and 6mm deep) in the welding seam

Cross hole (0.55mm diameter and 6mm deep) in the material

Fig. 26:   C-Scan image of the L-welded sample by EB welding

The analysis of the T-welded sample was performed both with straight-beam and angle beam adjustment. The specimen has a longitudinal hole (Ø 0.55 mm and 6 mm deep), from the welding area down through the base and three cross holes (Ø 0.55 mm and 6 mm deep). The positions of the artificial flaws are shown in Fig. 27.

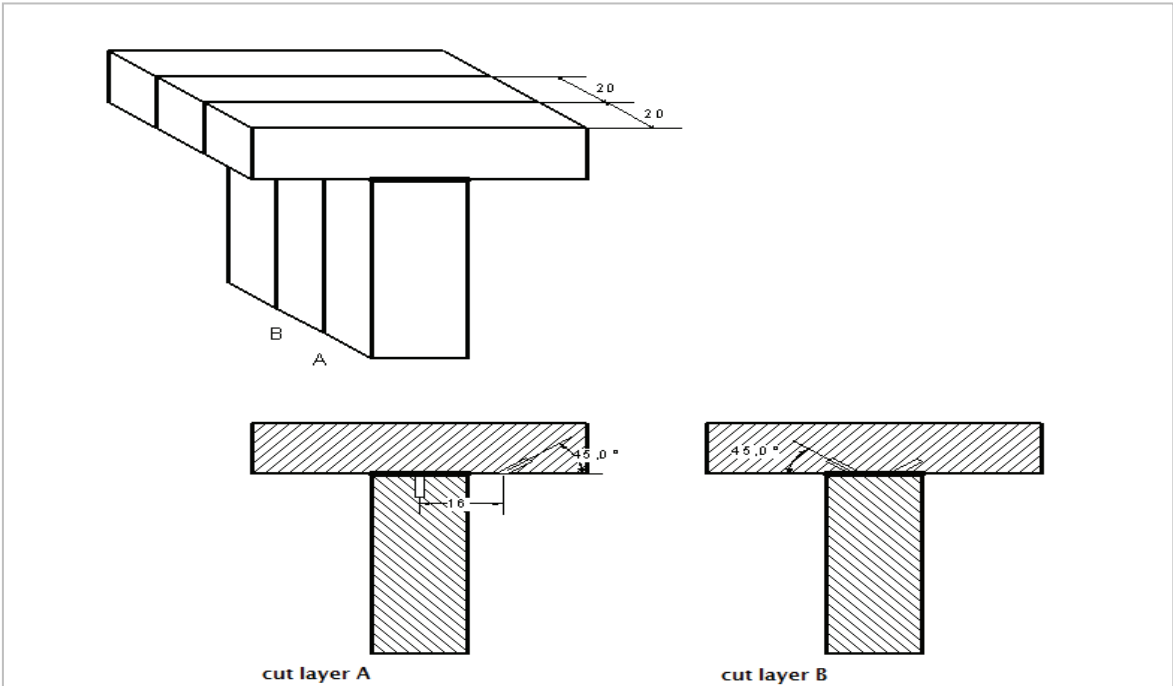

cut layer A

cut layer B

Fig. 27:   Sketch of the T-welded sample by EB welding

All holes were drilled before welding admitting clogging caused by weld-ups with the graphite lead. Using an amplification of 82 dB while applying different settings (angle of incidence changes and wavelength varies) and changing the direction of the scan, all registered flaws could be detected rather clearly (Fig. 28).
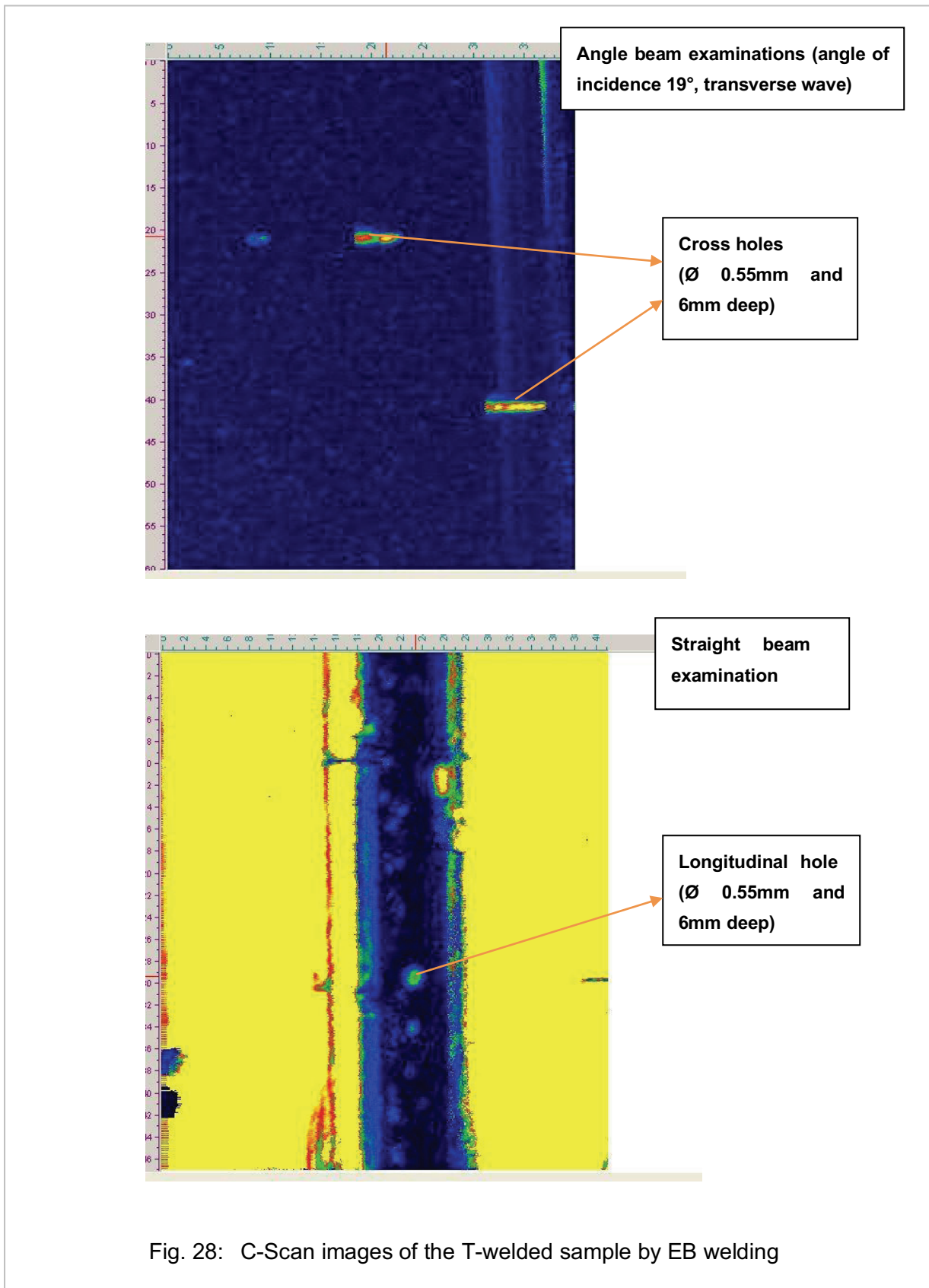
Angle beam examinations (angle of incidence 19°, transverse wave)

Cross holes (Ø 0.55mm and 6mm deep)

Straight beam examination

Longitudinal hole (Ø 0.55mm and 6mm deep)

Fig. 28: C-Scan images of the T-welded sample by EB welding

3.2.3 TIG Welding

The quality of the TIG-welded seams corresponded to that of the electron-beam welded ones, i.e. samples were stub-welded, L-welded and T-welded and were made from two EU-ROFER plates with artificially introduced flaws in and outside of the welding. Once again, a point-focused 15MHz encoder (type ISS) was used for ultrasonic testing.

The specimen tested first was a stub-welded sample where a graphite lead (0.5 mm in diameter), one tungsten wire (Ø 1.0 mm), and three cross holes each 0.5 mm in diameter had been drilled in the material from the V-joint preparation perpendicularly to the flank before welding. During the experiment, the specimen was examined using transverse waves at an amplification of 85 dB. As is evident from Fig. 29, the cross holes as well as the tungsten wire were clearly detectable and measurable. Just as in the case of the electron-beam welded seams, the graphite lead could not be detected. Probably it had been dissolved during welding.

Fig. 29: C-Scan image of the stub-welded sample by TIG welding
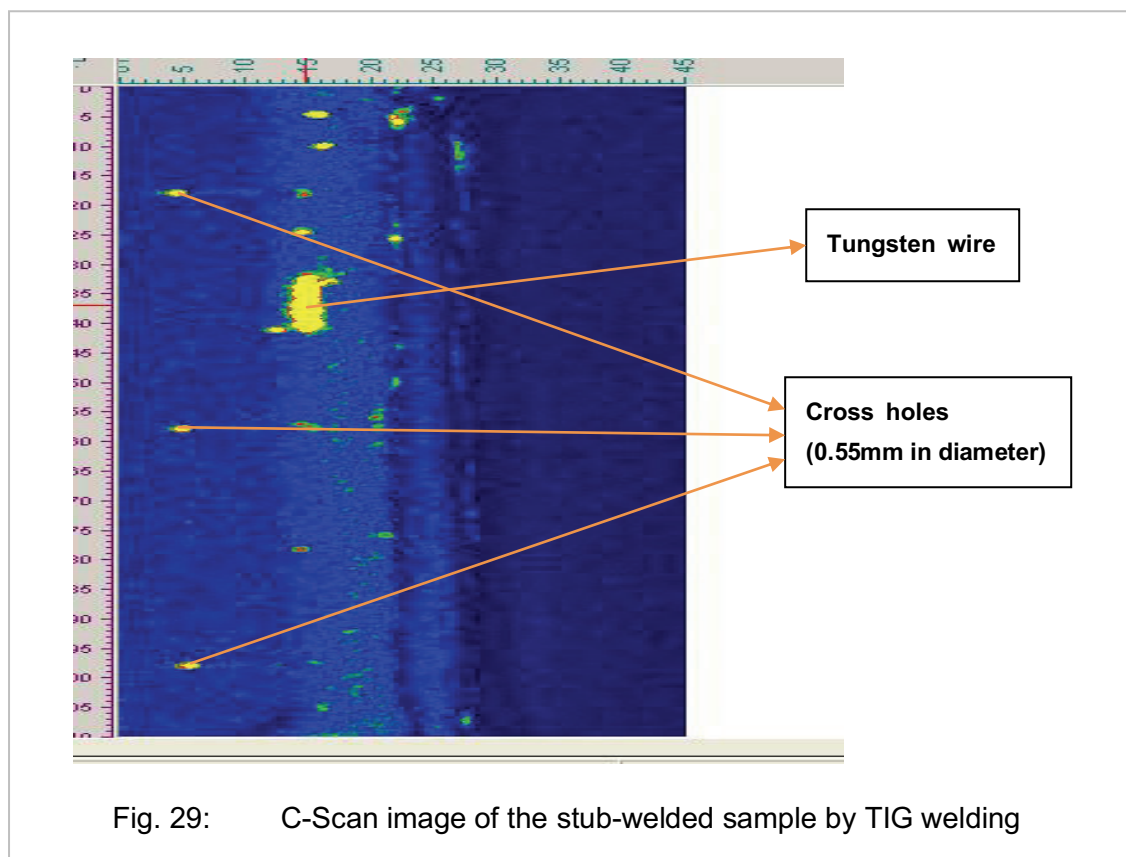
The positions of the artificially introduced flaws (holes - 0.55 mm in diameter and 6 mm deep) in an L-welded sample are shown in Fig.30.
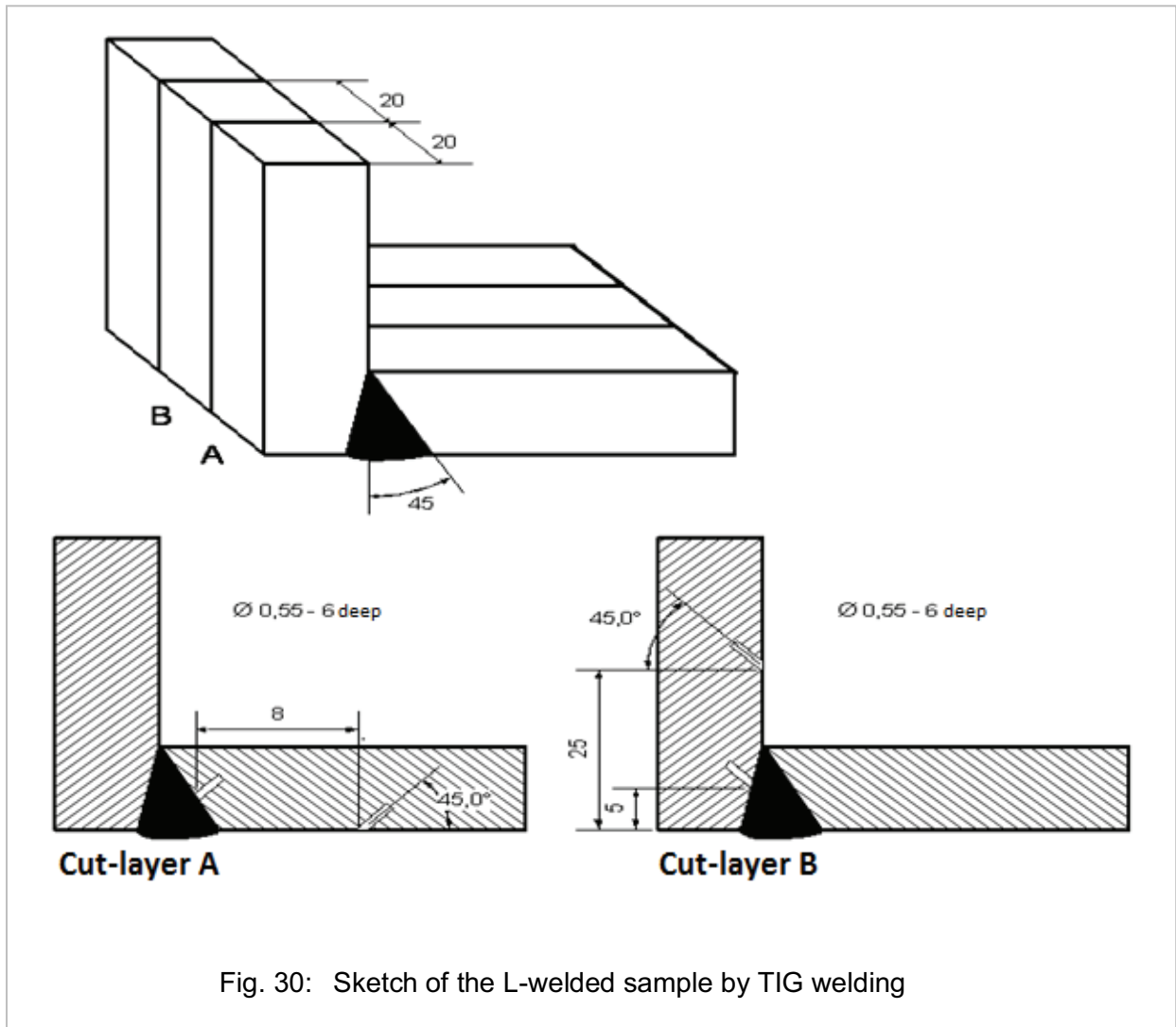

Fig. 30: Sketch of the L-welded sample by TIG welding

For identification of these artificial flaws the setting for transverse waves was used. All of the flaws prepared were detected by changing the direction of the scan and varying the position of the test object (Fig. 31). Amplification was at 82 dB.

Section A

Cross hole (0.55 mm in diameter and 6 mm deep) in the welding area

Section B

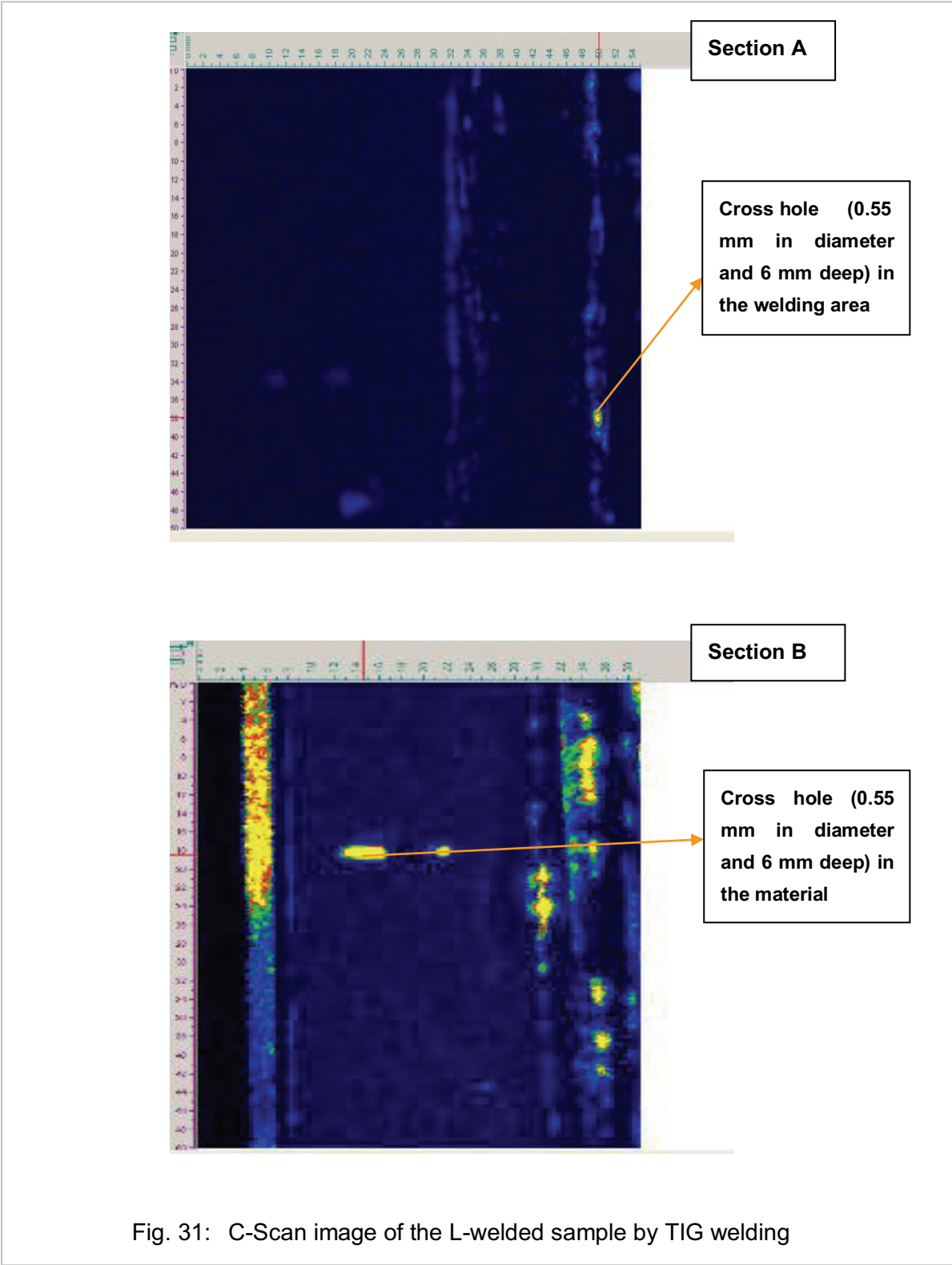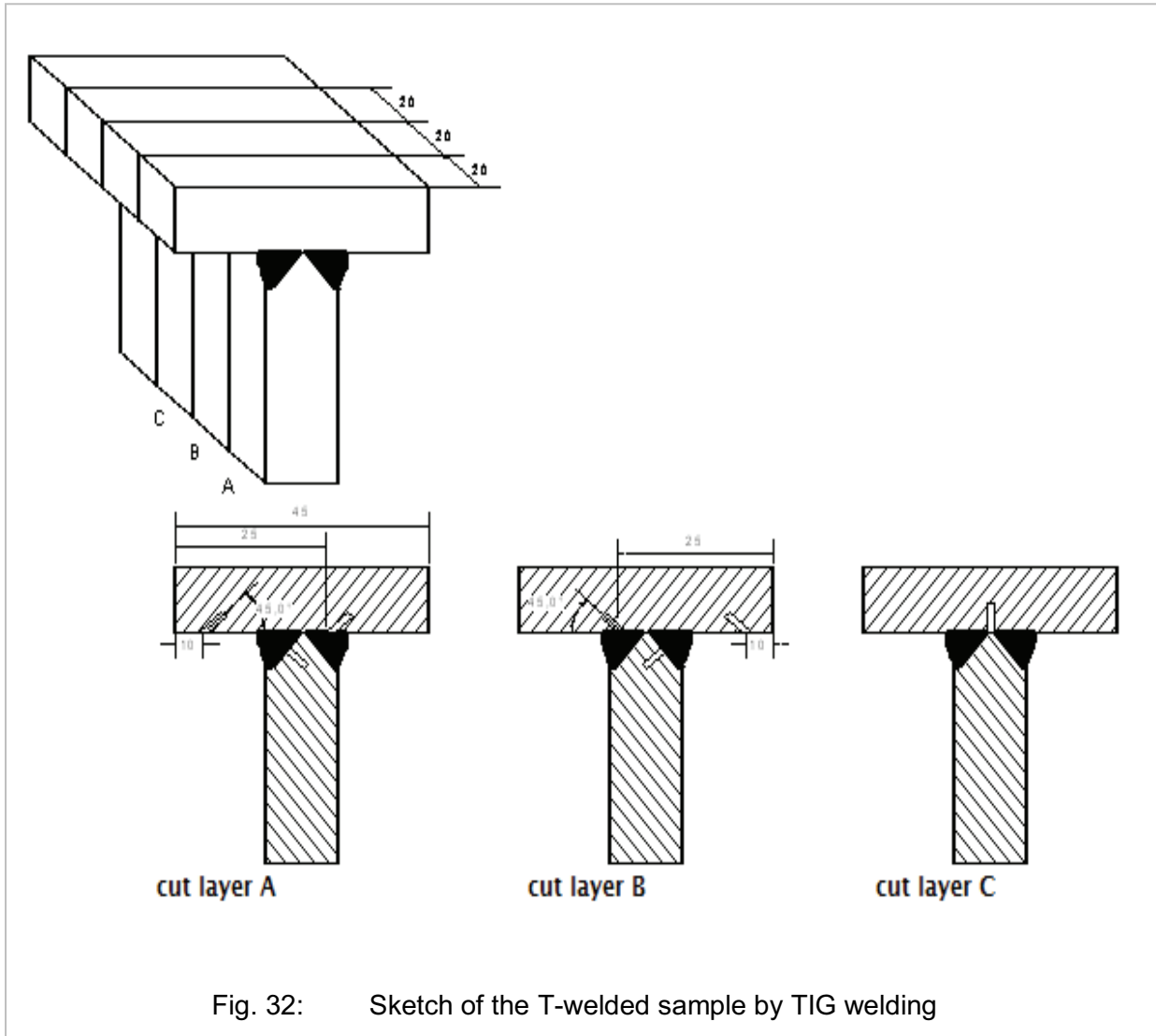Cross hole (0.55 mm in diameter and 6 mm deep) in the material

Fig. 31: C-Scan image of the L-welded sample by TIG welding

Next, a T-welded specimen with differently arranged cross holes (0.55 mm in diameter and 6mm deep) was scanned. Fig. 32 shows the sample view and the location of the holes.

cut layer A   cut layer B   cut layer C

Fig. 32:   Sketch of the T-welded sample by TIG welding

During ultrasound testing, the specimen was examined both with straight-beam and angle beam adjustments. The longitudinal (in the straight-beam examinations) and transverse (in the angle beam examinations) waves were energized. By changing the sensor positioning and varying the positions of the sample at amplification in the range of 80 – 82 dB, also these flaws were detected (Fig. 33).
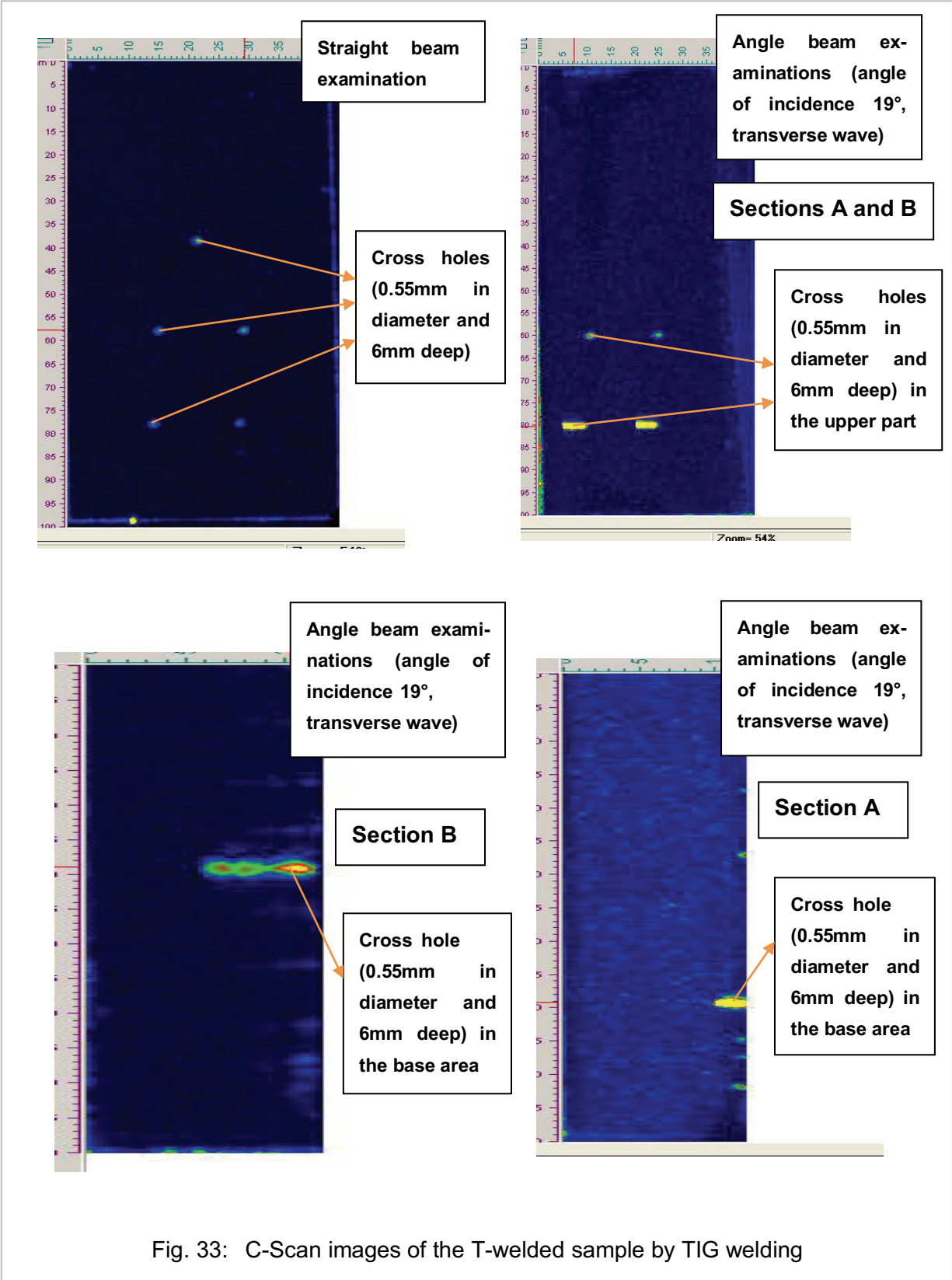
Straight beam examination

Cross holes (0.55mm in diameter and 6mm deep)

Angle beam examinations (angle of incidence 19°, transverse wave)

Sections A and B

Cross holes (0.55mm in diameter and 6mm deep) in the upper part

Angle beam examinations (angle of incidence 19°, transverse wave)

Section B

Cross hole (0.55mm in diameter and 6mm deep) in the base area

Angle beam examinations (angle of incidence 19°, transverse wave)

Section A

Cross hole (0.55mm in diameter and 6mm deep) in the base area

Fig. 33: C-Scan images of the T-welded sample by TIG welding

Finally, examinations were performed of the stub-welded specimen with two thin tungsten wires (0.5 mm and 0.2 mm in diameter) introduced directly into the welding area. Using different angle settings of the sensor and varying the wavelength, these two wires could be detected very well. Amplification during testing was in the range of 80 – 82 dB (Fig. 34, Fig. 35).
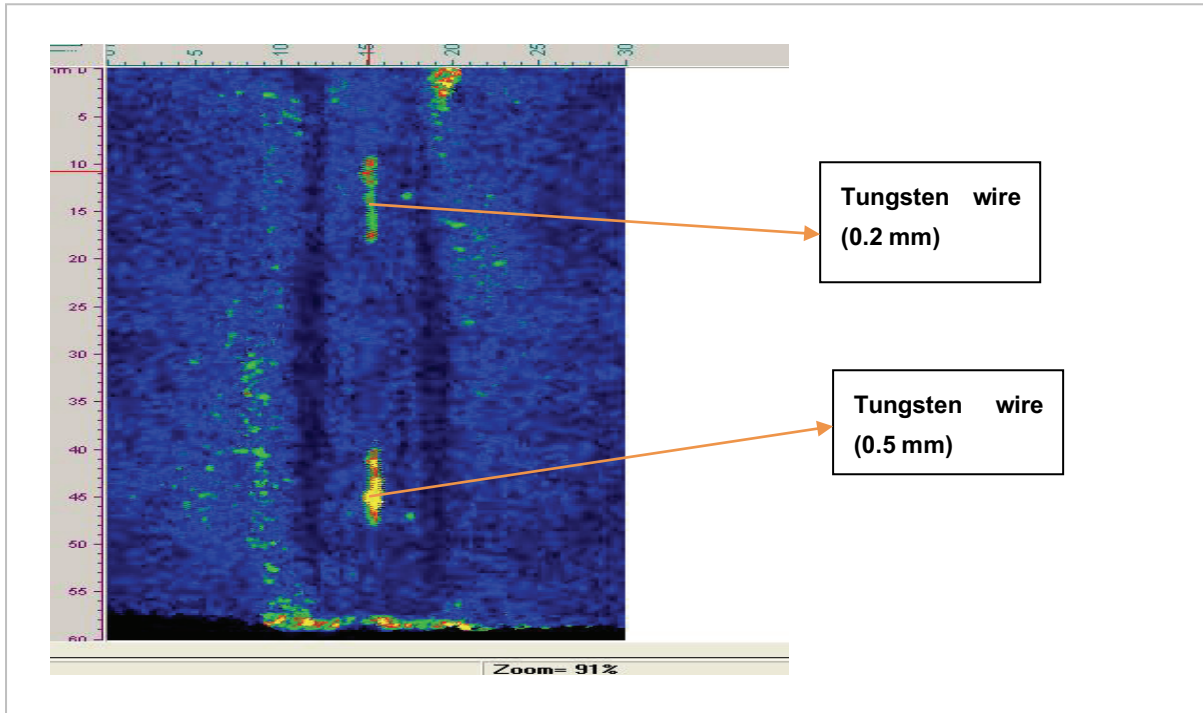

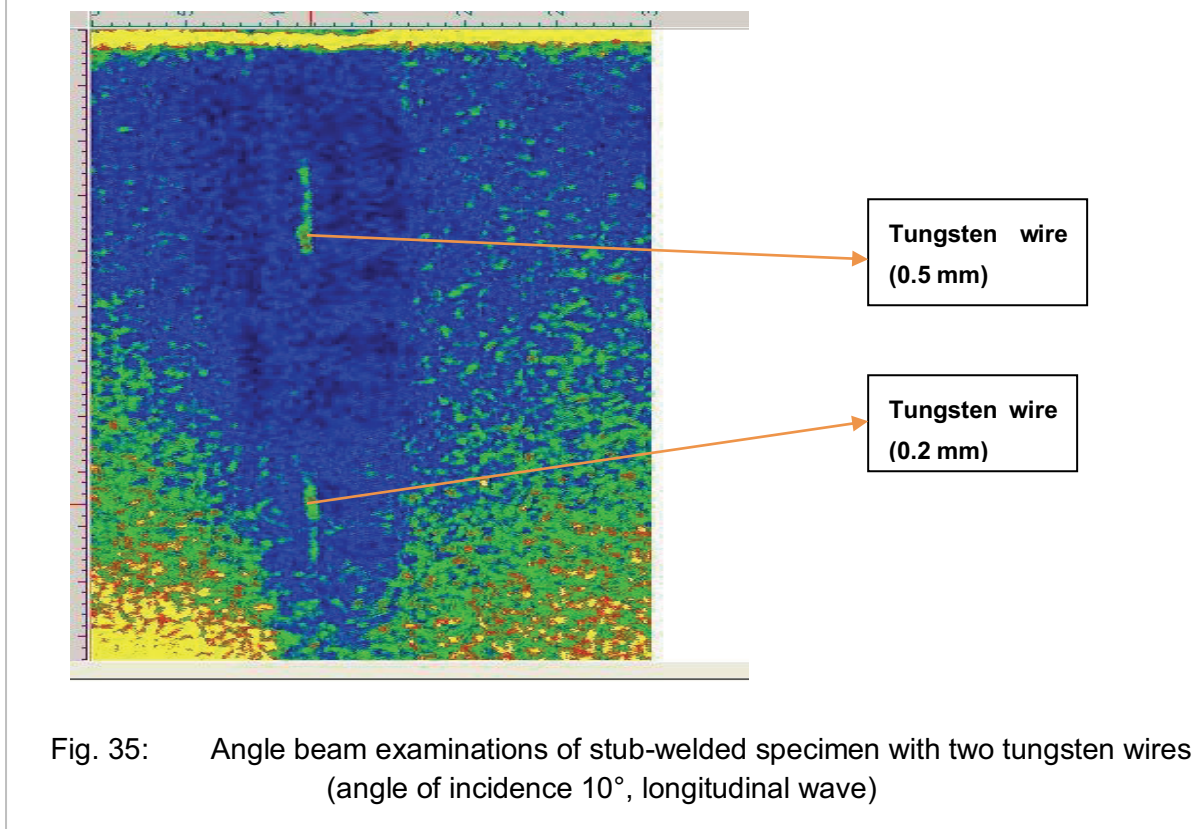Fig. 34:   Straight-beam examinations of stub-welded specimen with two tungsten wires

Fig. 35:   Angle beam examinations of stub-welded specimen with two tungsten wires
(angle of incidence 10°, longitudinal wave)

3.2.4 DAC (Distance Amplitude Correction) - Curve Production

A stage sample with inserted cross holes 0.2 mm and 0.1 mm in diameter was used as a reference block for DAC curve production (Fig. 36).

Fig. 36:   A stage sample for DAC-curve production
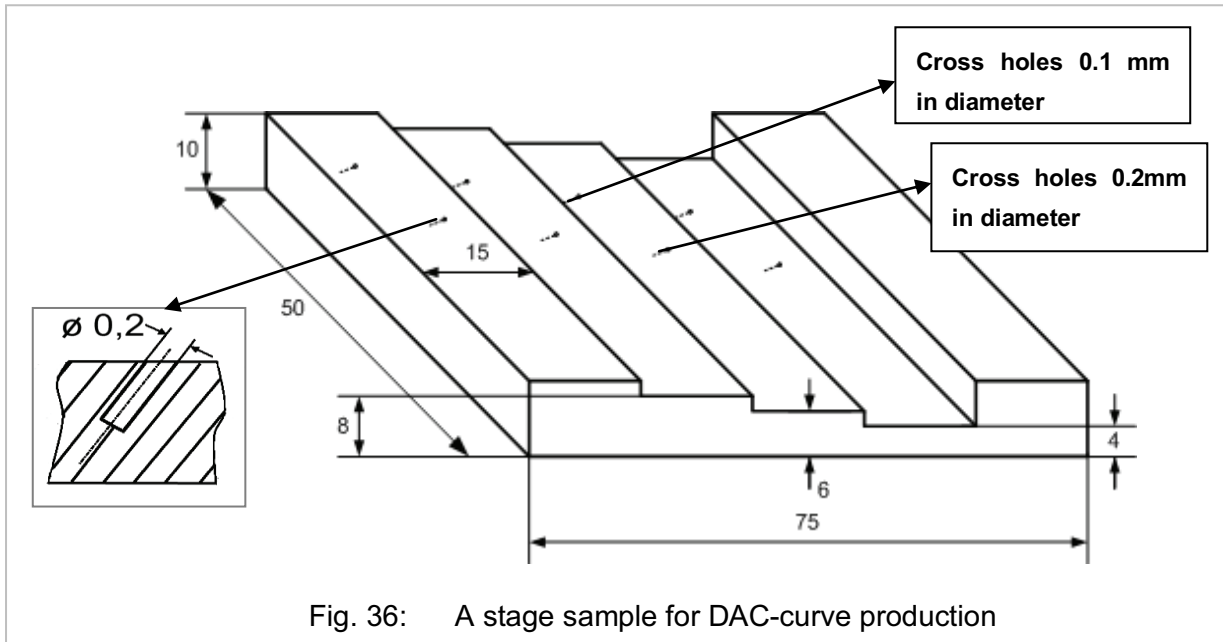
The DAC curve was generated for the 15 MHz sensor (type ISS) and for the transverse wave settings (angle of incidence 19°, transversal wave length). The amplification in the experiment was in the range of 70 – 72 dB. The DAC curves for the cross holes 0.2 mm in diameter are shown in Fig. 37.

Fig. 37   :   DAC- Curves
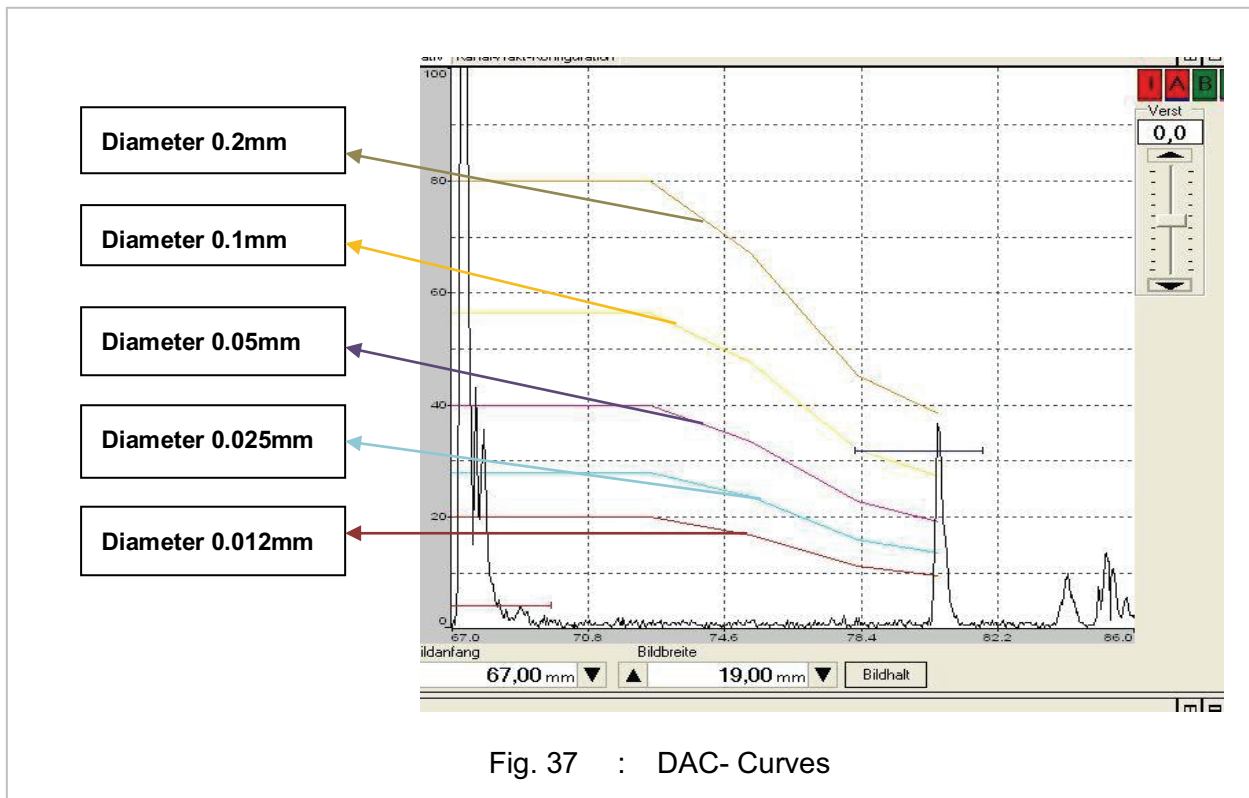
4 Conclusions

Application of the manual ultrasonic testing as well as the automated ultrasonic immersion technique enabled the examinations of EUROFER parts for blanket components of future fusion reactors including welding seams of the different types (diffusion welding, electron-beam welding and TIG-welding). In the context of this work the minimally visible flaw sizes have been determined in diverse types of welding joints for different welded samples.

- By manual ultrasonic testing the minimally visible flaw sizes in a diameter of 0.5 mm in the TIG- and EB- specimens can be detected.
- The application of the ultrasonic immersion technique allowed identification of the following flaw sizes:
    - In a diffusion-welded samples flaws of 0.1 mm in size can be detected provided that the distance from the wave entrance surface is of about 4 mm;
    - In TIG-welded and in electron-beam welded the flaws of 0.2 mm in size can be found.

DAC (Distance Amplitude Correction) curves were generated for flaws sized 0.2 mm and 0.1 mm in diameter. By using the decrease in amplification and generating several DAC curves (a multi-DAC curve), also very small flaws (down to e.g., 0.025 mm and 0.012 mm) might be evaluated.

5 Outlook

For further investigations of the welding joints from EUROFER, ultrasonic tests were considered for detection of even smaller flaws with sizes in the micrometer-range. To improve the quality assurance of the welded seams, other non-destructive methods e.g., X-raying and thermography, should be considered in addition. Application of the ultrasonic immersion testing for monitoring the process of the crack propagation in fracture mechanical bending specimens shall be investigated in the future.

6 Acknowledgment

7 IP reporting

All the works provided under the present task were according to the current state-of-the art. No foreground IPR has been produced under this task. All information from involved external

companies and sub-contractors is open and available, and no confidentiality or license agreement was signed. No invention or software development has to be declared.

8 References

[1] http://www.ndt.net/article/v04n09/erhard/erhard.htm

[2] http://www.ipeia.com/Misc_Docs/Thu%201115am%20Roux.pdf

[3] D. Volker, Die Ultraschall- Prüfung (1999)

[4] http://www.ndt-ed.org/EducationResources/CommunityCollege/Ultrasonics/Introduction/description.htm

[5] http://www.krautkramer.com.au/Nondestructive_Testing.pdf

[6] T. Ishii, N. Ooka, T. Hoshiya et.al. Journal of Nuclear Materials 307-311 (2002) 240-244.

[7] Krautkramer USD 15, Technical Reference and Operating Manual, English ID. 28578.

[8] F. Tavassoli, Fusion Demo Interim Design Criteria (DISDC) / Appendix A: Material Design Limit Data / A3.S18E Eurofer Steel, DMN Technical Report, DMN/DIR/NT/2004-000/A, 2004.

[9] http://www-civa.cea.fr/scripts/home/publigen/content/templates/show.asp?P=55&L=EN

[10] M. Berke, U. Hoppenkamps, Krautkrämer Training System, Tauchtechnikprüfung (2001)

[11] D. Döring, M. Rheinfurth, Universität Stuttgart, Institut für Kunststofftechnik, Ultraschall-Tauchtechnik (2009)

[12] http://www.ndt-ed.org/EducationResources/CommunityCollege/Ultrasonics/CalibrationMeth/DAC_Curve.htm

[13] GE Sensing & Inspection Technologie, Die Ultraschallprüfung (2009)

Annex A   UT results from GE Inspection Technologies (1)

GE Inspection Technologies

Prüfbericht:9616

GE Inspection Technologies GmbH   **Applikationslabor**

Robert-Bosch-Strasse 3   **Bearbeiter: T. Michalk**

D-50354 Hürth   **Datum:28.01.2008**

Prüfaufgabe: Ermittlung der Auflösbarkeit von Flachbodenbohrungen mit Durch-
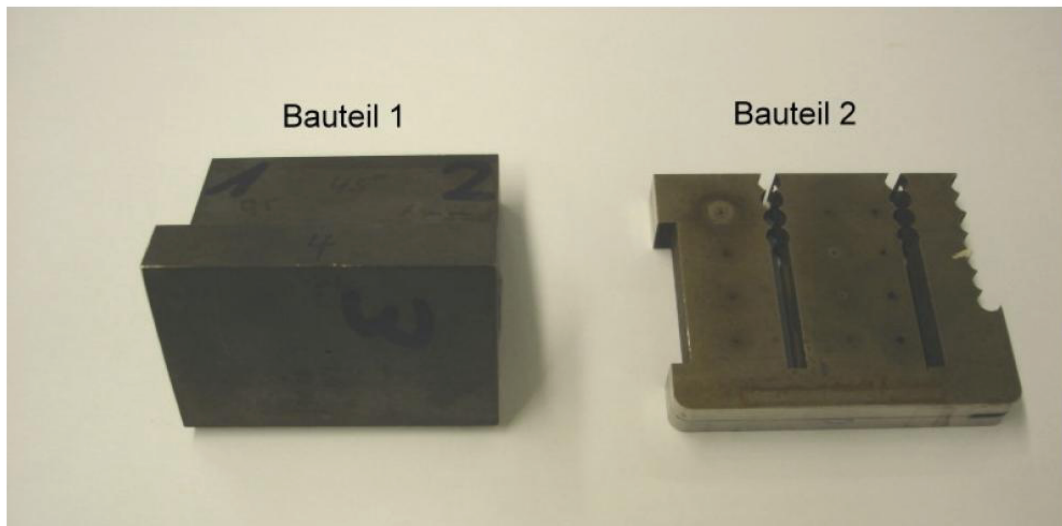messern von 0,4 mm bis 1,0 mm

Muster:

Abb. 1: Prüfmuster

Prüftechnik: Senkrechteinschallung mit Longitudinalwellen, Ankopplung direkt
(Bauteil 1) und in Tauchtechnik (Bauteil 2)

Prüfausrüstung: Ultraschallgerät: USD 15, USM 35
Prüfköpfe: IAP 10.6.3 [ID 57511] (Tauchtechnik)
                     H 15 MN 20 [ID 66054] (Tauchtechnik)
                     MB 4 S (Direktankopplung)
Zubehör: Tauchtechnik

GE Inspection Technologies

Prüfbericht:9616

Versuchsergebnisse

Bauteil 1

Die unter einem Winkel von 45° eingebrachten Flachbodenbohrungen können von der in der Zeichnung vermerkten Einschallposition nicht detektiert werden. Eine Auffindung wäre nur von der Unterseite des Bauteils möglich. Diese Einschallposition kann in der Praxis jedoch nicht realisiert werden. Somit fallen diese zwei Bohrungen bei den Untersuchungen aus.
Die senkrecht an der Unterseite eingebrachte Bohrung liefert, bei senkrechter Einschallung auf die Oberfläche, eine Fehleranzeige (Abb. 2), die deutlich von der Rückwandanzeige (Abb. 3) unterschieden werden kann.
Diese Untersuchung wurde mit direkter Ankopplung mit dem Prüfkopf MB 4 S durchgeführt.
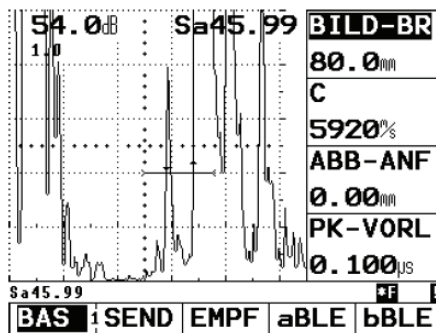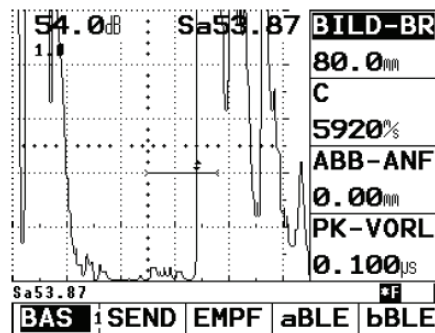

Abb. 2: Fehlerechoanzeige

Abb. 3: Rückwandechoanzeige

Bauteil 2

In diesem Bauteil ist mittig ein Kühlkanal eingebracht, der, je nach verwendetem Prüfkopf, hohe Anzeigen mit nachfolgend erhöhtem Rauschpegel erzeugt. Da eine Bohrung durch diesen Kühlkanal hindurch ragt, müssen zwei Auswerteblenden gesetzt werden und zwei unterschiedliche C-Bilder aufgezeichnet werden. Blende 1 bewertet den Bereich von der Oberfläche bis zum Kühlkanal, Blende 2 den Bereich vom Kühlkanalende bis zur Rückwand.
Die Untersuchung wurde zunächst mit dem punktfokussierten Prüfkopf IAP 10.6.3 durchgeführt. Die Ergebnisse werden in Form von farblich codierten C-Bildern dargestellt.
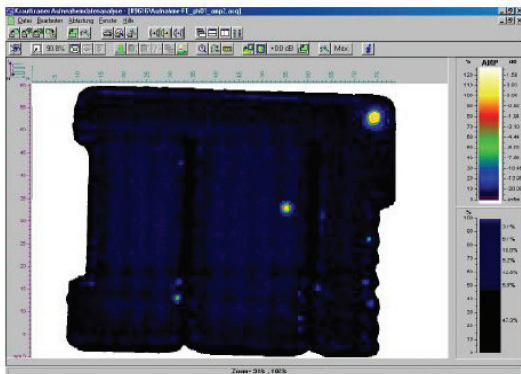
GE Inspection Technologies

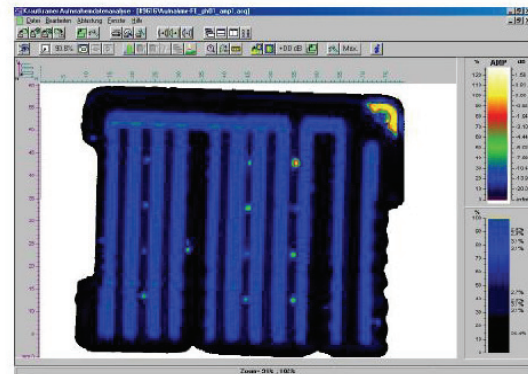Abb. 4: C-Bild Auswerteblende 1, 10 MHz

Abb. 5: C-Bild Auswerteblende 2, 10 MHz

Auf Grund der hohen Anzeigen des Kühlkanals wurden die Untersuchungen mit dem Prüfkopf H 15 MN 20 wiederholt. Dieser Prüfkopf verfügt über eine Frequenz von 15 MHz und einen Schwinger von 3 mm Durchmesser. Mit dieser Prüfanordnung erhält man folgende Ergebnisse:
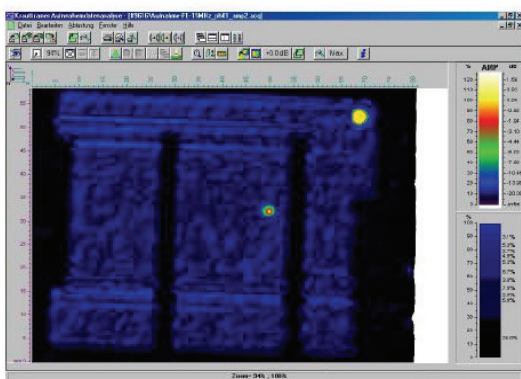

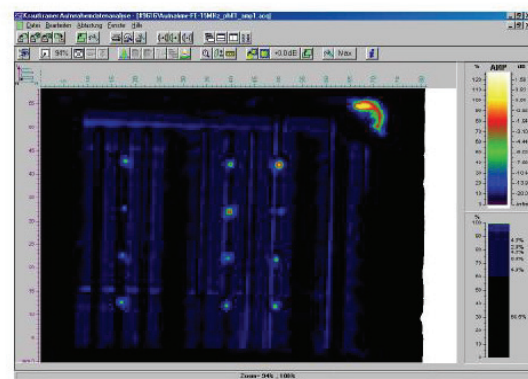
Abb. 6: C-Bild Auswerteblende 1, 15 MHz

Abb. 7: C-Bild Auswerteblende 2, 15 MHz

Im direkten Vergleich wird unter Verwendung des Prüfkopfes H 15 MN 30 eine schärfere Trennung der Fehleranzeigen von den Anzeigen des Kühlkanals erreicht. Des weiteren ist ein Amplitudengewinn von ca. 3dB zu verzeichnen.

Bemerkung:

Bauteil 1:
Für die manuelle Prüfung wird der Prüfkopf MB 4 S empfohlen. Soll dieses Bauteil in Tauchtechnik geprüft werden, so wird der Prüfkopf H 10 M empfohlen. Diese Empfehlungen gelten jedoch nur für die hier vorliegende Abmessung, also maximale Schallwege von ca. 55 mm.

Bauteil 2:
Hier sollte nur Tauchtechnik mit dem Prüfkopf H 15 MN 20 angewendet werden.

Annex B   UT results from GE Inspection Technologies (2)

GE Inspection Technologies   **Prüfbericht:9616a**

GE Inspection Technologies GmbH   **Applikationslabor**
Robert-Bosch-Strasse 3   **Bearbeiter: T. Michalk**
D-50354 Hürth   **Datum: 26.02.2008**

Anhang zum Bericht #9616 vom 28.01.2008

Prüfaufgabe: Nachweis von Zylinderbohrungen, die im Winkel von 45° in eine
Schweißnaht eingebracht sind

Prüftechnik: 45°-Winkeleinschallung mit Transversalwellen, direkte Ankopplung

Prüfausrüstung: Ultraschallgerät: USD 15
Prüfkopf: MSW-QC 10
Zubehör: Polystyrol-Vorlaufkörper für 45°-Transversalwelle
in Stahl (3250 m/s)

Versuchsergebnisse

Die Geometrie des Bauteils lässt eine Prüfung nur über eine Umlenkung zu, so dass die
Zylinderbohrungen in 0,75p getroffen werden. In Abbildung 1 ist das Prüfungsprinzip dar-
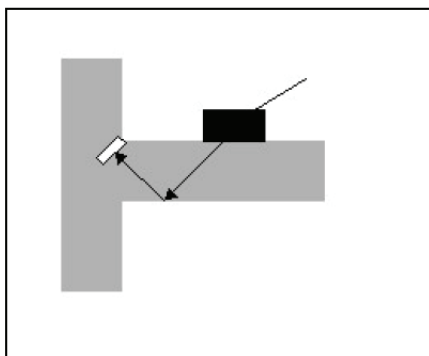gestellt.

Abb. 1: Prüfprinzip der Winkeleinschallung

GE Inspection Technologies

Prüfbericht:9616a

Eine direkte Einschallung auf die Zylinderbohrung, also ohne Umlenkung, ist wegen der Breite der Schweißnaht nicht möglich. Der Prüfkopf kann dadurch nicht nah genug an die Bohrungen herangeführt werden.
Die Prüfergebnisse zeigen, dass die Umlenkung des Schallstrahls Anzeigen von den Zylinderbohrungen mit ausreichend großem Signal-Rauschabstand liefert.
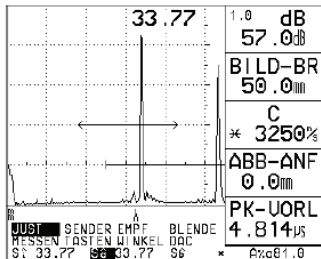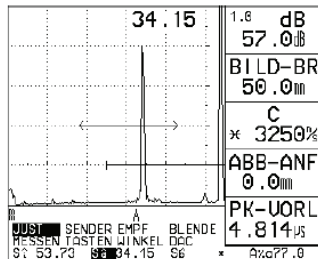

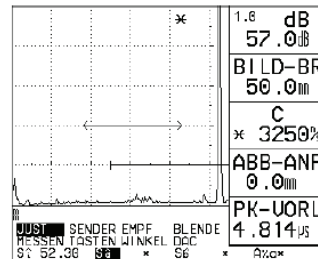Abb. 2: Bohrung Nr. 1   Abb. 3: Bohrung Nr. 2   Abb. 4: Schweißnaht ohne Bohrung

Die Abbildungen 2 und 3 zeigen die Anzeigen der Zylinderbohrungen, Abbildung 4 zeigt einen fehlerfreien Bereich der Schweißnaht. Die Bohrungen können klar detektiert werden.

The ferritic-martensitic steel EUROFER is intended for use as a structural material for blanket components of future fusion reactors. A blanket module consists of a multiplicity of diffusion-welded cooling plates, which are connected by TIG, EB or laser welding seams. For the quality assurance of these welding seams the ultrasonic non-destructive testing is currently examined. In the context of this work the manual testing and the ultrasonic immersion testing are considered for the examination of EUROFER parts including welding seams of different types (diffusion welding, electron-beam welding and TIG – welding). Differently arranged artificial flaws of varying sizes were introduced into the welding seams to determine their minimum detectable size. In essence, the artificially introduced flaws for immersion testing consisted of longitudinal holes and cross holes 0.2 mm to 1.0 mm in diameter as well as of tungsten wires whose diameter was in the range of 0.2 mm to 1.0 mm. For manual testing holes were introduced with a diameter of 0.5 mm only. Investigations were conducted using the KC 200 immersion testing facility developed by GE Inspection Technologies and the USD 15s by Krautkramer for manual scanning. Ultrasonic testing was performed intermitting straight- and angle beam examinations of longitudinal and transverse waves from sensors of different resolutions. The DAC (Distance Amplitude Correction) curves for flaws that are 0.2 mm and 0.1 mm in diameter were derived from the measuring results in addition.